Parallel Virtual Screening to Discover Phytocompounds to Counter the Resistance Inducing Effect of Double Mutations in MDR Tuberculosis

A Major Project dissertation submitted in partial fulfillment of the requirement for the degree of

Master of Technology

In

Bioinformatics

Submitted by

Kunal Patel
(Roll No.: 2K12/BIO/12)

Delhi Technological University, Delhi, India
Under the supervision of

Dr. Navneeta Bharadvaja

Department of Biotechnology
Delhi Technological University
(Formerly Delhi College of Engineering)
Shahbad Daulatpur, Main Bawana Road, Delhi-110042, India

CERTIFICATE

This is to certify that the M. Tech dissertation entitled **"Parallel Virtual Screening to Discover Phytocompounds to Counter the Resistance Inducing Effect of Double Mutations in MDR Tuberculosis."**, submitted by **Kunal Patel (Roll No.: 2K12/BIO/12)** in partial fulfillment of the requirement for the award of the degree of Master of Technology, Delhi Technological University (formerly Delhi College of Engineering), is an authentic record of the candidate's own work carried out by him under my guidance.

The information and data enclosed in this dissertation is original and has not been submitted elsewhere for honoring of any other degree.

Date: July 30, 2014

Dr. Navneeta Bharadvaja
Assistant Professor
Department of Biotechnology
Delhi Technological University
(Formerly Delhi College of Engineering, University of Delhi)

DECLARATION

I, **Kunal Patel**, hereby declare that the work entitled **"Parallel Virtual Screening to Discover Phytocompounds to Counter the Resistance Inducing Effect of Double Mutations in MDR Tuberculosis."** has been carried out by me under the guidance of Dr. Navneeta Bharadvaja, in Delhi Technological University, Delhi.

This dissertation is part of partial fulfillment of requirement for the degree of M.Tech in Bioinformatics. This is the original work and has not been submitted for any other degree in any other university.

Kunal Patel

Roll No.: 2K12/BIO/12

ACKNOWLEDGEMENT

I would like to acknowledge my deep sense of gratitude to ***Prof. B. D Malhotra, (Head of Department) Department of Biotechnology, Delhi Technological University, Delhi -110042*** *for giving me an opportunity to study and work in this prestigious Institute.*

I am extremely thankful to my mentor, ***Dr. Navneeta Bharadvaja****,* ***Assistant Professor, Department of Biotechnology, Delhi Technological University, Delhi-110042*** *for her exemplary guidance, monitoring and constant encouragement throughout the M. Tech course. I would also like to thank her for sparing the efforts in compiling the work presented here.*

I wish to express my sincere gratitude to ***Dr. Abhinav Grover, Assistant Professor, School of Life Sciences, Jawaharlal Nehru University, Delhi -110067*** *for providing me continuous support throughout this project.*

At last, I am extremely thankful to my parents, family members and friends specially Jaspreet Kaur and Chakshu Vats whose blessings and support were always with me.

KUNAL PATEL

Roll No.: 2K12/BIO/12

LIST OF FIGURES

Figure 1: Nucleotide sequence and missense mutations within the QRDRs of gyrA.

Figure 2: Workflow for the present study

Figure 3: High Burden Countries according to WHO data

Figure 4: Classification of tuberculosis on the basis of resistance Figure 2:

Figure 5: N terminal helix blocking the path of drug by covering the bing site of Ofloxacin.

Figure 6: Domain organization and structures of the individual domains from the *M. tuberculosis* DNA gyrase catalytic core.

(A). Domain organization of the *M. tuberculosis* DNA gyrase.

(B) Two views of the dimeric breakage-reunion domain from *M. tuberculosis* colored by regions. The crystal structure of the complete breakage-reunion domain (GA57BK) extends from D9 to A501. The N-terminal helix is colored in Yellow, the DNA-gate containing the catalytic residues R128 and Y129 and the QRDR-A in blue, rest protein in green.

(C) Domain organization of breakage-reunion domain (GA57BK)

Figure 7: Structure of Chebulinic Acid

Figure 8: RMSD AND RMSF plot of Wild type DNA gyrA Chain A enzyme after double point mutation, energy minimization and simulation.

Figure 9: RMSD AND RMSF plot of 90V94G DNA gyrA Chain A enzyme after double point mutation, energy minimization and simulation.

Figure 10: RMSD AND RMSF plot of 74S94G DNA gyrA Chain A, enzyme after double point mutation, energy minimization and simulation.

Figure 11: RMSD AND RMSF plot of 90V91P DNA gyrA Chain A enzyme after double point mutation, energy minimization and simulation.

Figure 12: RMSD AND RMSF plot of Wild type DNA gyrA Chain A enzyme after docking and simulation.

Figure 13: RMSD AND RMSF plot of 90V94G DNA gyrA Chain A enzyme after docking and simulation.

Figure 14: RMSD AND RMSF plot of 74S94G DNA gyrA Chain A, enzyme after docking and simulation.

Figure 15: RMSD AND RMSF plot of 90V91P DNA gyrA Chain A enzyme after docking and simulation.

Figure 15: H- bond and hydrophobic interaction.

(A) Hydrogen bond interaction between CA and binding cavity of Wild type DNA gyrA chain A (represented in green colour)

(B) Hydrophobic interactions interaction between CA and binding cavity of Wild type DNA gyrA chain A (represented in green colour)

Figure 16: H-bond and Hydrophobic interaction.

(A) Hydrogen bond interaction between CA and binding cavity of 90V94G DNA gyrA chain A (represented in green colour)

(B) Hydrophobic interactions interaction between CA and binding cavity of 90V94G DNA gyrA chain A (represented in green colour)

Figure 17: H-bond and Hydrophobic interaction.

(A) Hydrogen bond interaction between CA and binding cavity of 74S94G DNA gyrA chain A (represented in green colour)

(B) Hydrophobic interactions interaction between CA and binding cavity of 74S94G DNA gyrA chain A (represented in green colour

Figure 18: H-bond and Hydrophobic interaction.

(A) Hydrogen bond interaction between CA and binding cavity of 74S94G DNA gyrA chain A (represented in green colour)

(B) Hydrophobic interactions interaction between CA and binding cavity of 74S94G DNA gyrA chain A (represented in green colour)

Figure 19: Stearic hindrance between DNA strand at DNA gate and distance between catalytic Tyrosine 129 residue and Phosphate group of DNA in Wild type DNA gyrase A chain A before (Blue) and after (Red) docking and simulation

Figure 20: : Stearic hindrance between DNA strand at DNA gate and distance between catalytic Tyrosine 129 residue and Phosphate group of DNA in 90V94G DNA gyrase A before (Blue) and after (Red) docking and simulation

Figure 21: Stearic hindrance between DNA strand at DNA gate and distance between catalytic Tyrosine 129 residue and Phosphate group of DNA in 74S94G DNA gyrase A chain A before (Blue) and after (Red) docking and simulation

Figure 22: Stearic hindrance between DNA strand at DNA gate and distance between catalytic Tyrosine 129 residue and Phosphate group of DNA in 90V91P DNA gyrase A chain A before (Blue) and after (Red) docking and simulation

LIST of TABLES

Table 1: Binding cavity size and area

Table 2: Top five compounds with their docking score against wild and mutant type DNA gyrase enzyme

Table 3: Link to database for top five common inhibitor.

Table 4: RMSF data of wild and mutant strains pre Docking and MD.

Table 5: RMSF data of wild and mutant strains post Docking and MD.

Table 6: RMSD data of wild and mutant strains pre Docking and MD for 12ns.

Table 7: RMSD data of wild and mutant strains post Docking and MD for 16ns.

LIST OF ABBREVIATIONS

ADC	L-Aspartate a-decarboxylase
AIDS	Acquired Immunodeficiency Syndrome
AMK	Amikacin
BCG	Bacillus of Calmette and Guérin
BCR-ABL	Breakpoint Cluster Region-Abelson Enzyme
CAP	Capreomycin
CA	Chebulinic Acid
CML	Chronic Myelogenous Leukemia
DAP	Diaminopimelic Acid
DHDPS	Dihydrodipicolinate synthase
DNA	Deoxyribonucleic Acid
DOTS	Directly Observed Treatment Short course
DR-TB	Drug resistant Tuberculosis
EIS	Enhanced Intracellular Survival
HBC	High Burden Countries
HIV	Human Immunodeficiency Virus
HTVS	High Throughput Virtual Screening
HTS	High Throughput Screening
INH	Isoniazid
KAN	Kanamycin
L-BFGS	Low-memory Broyden- Fletcher- Goldfarb
MDR-TB	Multi drug resistant Tuberculosis
MD	Molecular Dynamics
MRSA	Meticillin resistant Staphylococcus aureus
Mtb	*Mycobacterium tuberculosis*
MtPncA	Mycobacterial Pyrazinamidase
NGS	Next Generation Sequencing
OPLS	Optimized Potentials for Liquid Simulations
PBP	Penicillin binding proteins
PDB	Protein Data Bank
PncA	Pyrazinamidase
POC	pyrazonic acid
PPC	N-phenylpyrazine-2-carboxamide
PTB	Pulmonary TB
PZA	Pyrazinamide
RMP	Rifampicin
RO5	Lipinski rule of 5
SBDD	Structure-Based Drug Discovery
TDR-TB	Total drug resistant Tuberculosis
XDR-TB	Extentsive drug resistant Tuberculosis
XP	Extra Precision Docking

90V94G	Ala90Val + ASP94Gly
74S94G	Ala74Ser + ASP94Gly
90V91P	Ala90Val + Ser91Pro

CONTENTS

S. No	Tile	Page
	LIST OF FIGURES	iv
	LIST OF TABLES	vi
	LIST OF ABBREVIATIONS	vii
1	ABSTRACT	1
2	INTRODUCTION	2
3	REVIEW OF LITERATURE	4
3.1	Multi-drug-resistant and extensively drug-resistant tuberculosis	5
3.2	Mechanism causing Quinolone resistance in M. tuberculosis.	7
3.2.1	Resistance conferred due to Genetic mutation	7
3.2.2	Resistance conferred due to Molecular mimicry of drug targets	8
3.2.3	Mutation inducing resistance against Quinolones class of drugs	9
3.3	Why target DNA Gyrase?	10
3.4	HTVS as means of new drug candidate identification	12
3.5	Significance of Phytocompounds in drug discovery	14
3.6	Application of HTVS Leading To Hit Identification	15
4	METHODOLOGY	19
4.1	Preparation of wild type and mutated DNA Gyrase A structures	19
4.2	Binding cavity prediction	19
4.3	Virtual library preparation for HTVS	20
4.4	High throughput virtual screening and docking studies	22
4.5	Molecular dynamics simulations of ligand-bound complexes	23
5	RESULTS AND DISCUSSION	24
5.1	Binding cavity prediction	24
5.2	High Throughput virtual screening and XP docking studies	24
5.3	Molecular dynamics simulations studies	26
5.4	Effect of Chebulinic acid (CA) on the distance between catalytic residue Tyr129 and phosphate group from DNA	33
5.5	Stearic hindrance at C-gate of DNA gyrase A	33
6	CONCLUSION AND FUTURE PERSPECTIVE	38
7	REFERENCES	39
8	APPENDIX	44

Parallel Virtual Screening to Discover Phytocompounds to Counter the Resistance Inducing Effect of Double Mutations in MDR Tuberculosis.

Kunal Patel

Delhi Technological University, Delhi, India

1 ABSTRACT

Drug resistant tuberculosis has threaten all the advances made in tuberculosis control at the global stage in the last few decades. Resistance to quinolone class of drug like Ofloxacin which are being used as a main drug for multiple drug resistant tuberculosis treatment have given rise to cases of extensive drug resistant tuberculosis. DNA gyrase enzyme, essential for DNA replication, translation, and transcription are targeted by quinolones for their bactericidal effect and can be an excellent target for antibacterial drug discovery. Mutations in quinolone resistance determining region of gyrase enzyme, especially in gyrA subunit have conferred resistance to quinolones based drugs. Here we report, a successful application of High Throughput Virtual Screening (HTVS) in identification of a common inhibitor for both wild type and mutant type Mycobacterium DNA gyrase. The most prevalent double mutant strain of tuberculosis that were targeted here is 90V94G, 74S94G and 90V91P DNA gyrase. Chebulinic Acid (CA), a phytocompound obtained from *Terminalia chebula* was the outcome of present HTVS study as a most potent inhibitor. Also, four more compounds were identified along with CA from a virtual library of 1, 79,299 compounds, but they were less potent compared to CA. CA scored high Extra Precision docking score i.e. -14.63, -16.46, 15.94 and -15.11 against wild type and 90V94G, 74S94G and 90V91P double mutants respectively. The complex was stabilized by multiple H bonding and numerous hydrophobic interaction. This was shown by molecular dynamics simulation studies for a period of 16ns, lower root mean square deviation (RMSD) value and lower root mean square fluctuation (RMSF) value of residues interacting with ligand indicated a formation of stable complexes in all the four cases. The dual inhibition mechanism seems to be pretty effective as CA is causing displacement of catalytic tyr129 residue from 1.6A□ to 7.3 A□ from its target phosphate molecule. Also, the CA is causing stearic hindrance to DNA strand at the DNA gate site resulting in loss of cleavage and religation activity of the enzyme. This phytocompound displays desirable quality for carrying forward as a lead compound for drug development.

2 INTRODUCTION

Mycobacterium tuberculosis causes one of the most severely affecting human disease called Tuberculosis. The bacteria mostly target the lungs, but it can also infect other body parts. Both diagnosis and treatment still pose a great challenge to the human community. With the present duration of treatment time, which is quite long and inappropriate use of the first line of tuberculosis drugs has led to the emergence of drug resistant *Mycobacterium tuberculosis* strains. Drug resistant TB has started to threaten all the advances we have made in TB control at global stage in the last few decades (WHO 2013). In 2012, according to the WHO report, 750 000 cases of multidrug-resistant (MDR) TB were reported. Apart from that MDR TB, 92 countries have also reported cases of Extensively drug-resistant (XDR) TB (WHO 2013). Both MDR TB and XDR TB are considered as a disease with very high mortality rates and near about 170,000 MDR-TB deaths have been reported in 2012 (WHO 2013). China, India, and the Russian Federation are considered as a hotspot zone for the disease as more than one half of these cases have occurred here (WHO October, 2013). In case of MDR-TB, WHO advocates Fluoroquinolone drugs like Ofloxacin when resistance to at least two drugs rifampicin and isoniazid is proven (Walwaikar, Morye et al. 2003). However threat to this drug have been posed by increase in the number of Fluoroquinolone resistance cases.

A study was conducted by Shi et al 2003 on 109 clinical isolates and 87 samples of them occurred to be Fluoroquinolone resistant. On sequencing the QRDR region of DNA, it was revealed that mutations are predominantly occurring at specific positions of gyrA i.e. at codons 90, 91, and 94. At 94 position, four different types of point mutations were reported (Asp94 to Gly, Ala, Tyr, and Asn) (Shi, Zhang et al. 2006) (Fig: 1). Most unique observation of this study was that 49 isolates of the 87 Ofloxacin-resistant isolates (56%) had double point mutations. Discovery of Double point mutation in DNA gyrA was thought to be relatively rare (Xu, Kreiswirth et al. 1996, Cheng, Yew et al. 2004) and is not expected to be observed frequently in clinical isolates. So, the high rate at which these double point mutations were observed in gyrA and Ala74Ser mutation shows the development of Fluoroquinolone resistance after prolonged Fluoroquinolone exposure. A real threat of development of extensively drug-resistant (XDR) strains has been posed by the findings of this study (Sun, Zhang et al. 2008, van Doorn, An et al. 2008, An, Duyen et al. 2009).

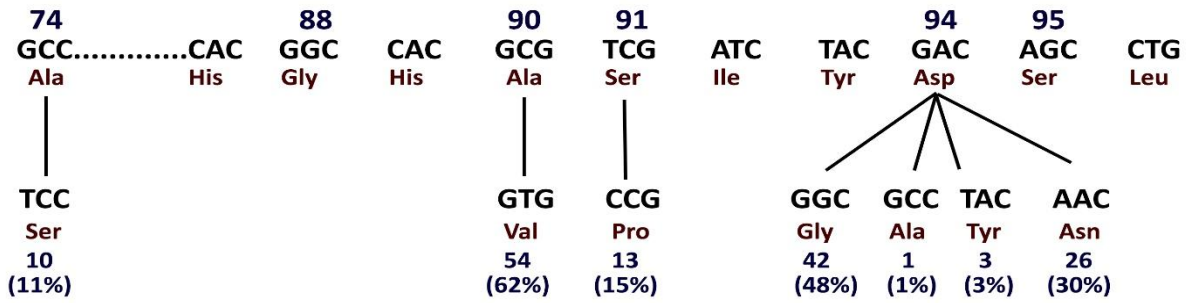

Figure 1: Nucleotide sequence and missense mutations within the QRDRs of gyrA.

Aim of the present work

The overall aim of taking this study is to apply different modern computational methods for identification of hits for early drug discovery phase and for developing novel inhibitors for the crucial tuberculosis enzyme DNA gyrase in wild type *M. tuberculosis* and their three most prevalent double mutants. Since DNA gyrase is an established and effective target for TB control with negligible side effects. We have chosen this enzyme as a target and tried to overcome the resistance by the screening of a virtual library of 1, 79,299 compounds to find lead compounds which are can inhibit DNA gyrase's wild type as well as its resistant strains. The workflow adopted is explained in Fig: 2.

The specific objectives were:

- To identify a new binding site to overcome the effects of mutations as they were restricting the access of Quinolone drugs to the binding cavity and conferring resistance to drug using Q-SiteFinder server (Laurie and Jackson 2005).
- To identify a common natural inhibitors having the potential to inhibit both wild type and mutant Quinolone drug resistant strains of DNA gyrase using parallel High Throughput Screening technique.
- To validate the affinity of common inhibitor and stability of the compound-enzyme complex by extra precision docking and Molecular Dynamic simulation.
- To present inhibition mechanism for the proposed lead compound.

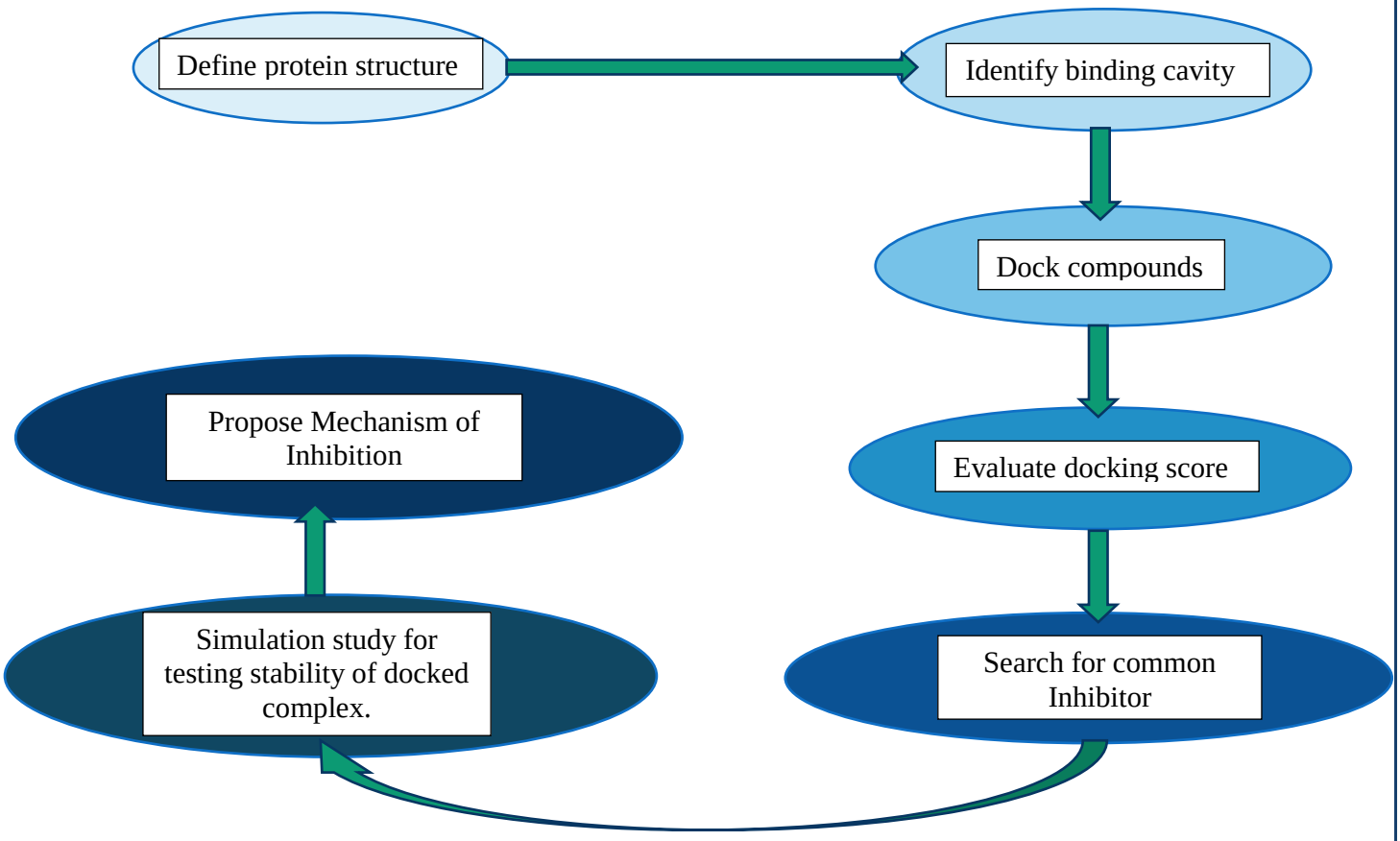

Figure 2: Workflow for the present study

3 REVIEW OF LITERATURE

Tuberculosis (TB) is a grave infectious disease caused mainly by *Mycobacterium tuberculosis*. Very often lung is the primary target of this bacteria and causes Pulmonary TB (PTB). However, it can also affect several other organs like lymph glands, intestine, meninges, bones, joints, skin and other tissues of the body. Although *M. tuberculosis* is the main cause for the maximum number of TB cases but clinical evidences of involvement of various other species of *Mycobacterium* like *M. fortuitum*, *M. avium*- intracellulare complex (MAC), and *M. smegmatis* in pathogenesis of the disease has been found. The disease is chronic in nature and the patient shows persistent cough, discontinuous fever, and loss of appetite, weight loss, chest pain and haemoptysis as the basic symptoms (Park 2007). TB and human share a long period of coevolution, perhaps of several million years (Gutierrez, Brisse et al. 2005). As old as 9000 yrs., Human remains showing signs of tuberculosis has been recovered (Hershkovitz, Donoghue et al. 2008). Even the bones of Neolithic man recovered from different parts of the world has shown evidence of TB. Also, from the graves of ancient Egypt various recovered mummified bodies have shown positive evidence of TB in the spine. These evidence shows that the human species have suffered from TB as early as in 5000 BC (Donoghue, Marcsik et al. 2005).

In the Indian context, evidences of TB have been traced to 300BC. TB is a highly contagious disease and spread from the droplets of cough from throat of people who are suffering from active tuberculosis. After the scientist Koch, TB is also known as Koch's disease. Koch was the first scientist to identify *Mycobacterium tuberculosis* as a causative agent of tuberculosis on 24 March 1882 (Al-Sharrah 2003). The first vaccine known as BCG was developed from attenuated bovine-strain tuberculosis by Albert Calmette and Camille Guerin in 1906 (Bonah 2005). Presence of Tuberculosis is very frequent in healthy people, but it is present in latent phase and mostly produces no symptoms as the person's immune system acts to "wall off" the bacteria (Migliori, Loddenkemper et al. 2007). Tuberculosis affects a large number of people as one third of the world's population is thought to be infected with *M. tuberculosis* and the numbers are continuously increasing with the rate of one person per minute (WHO October, 2013). It's present mostly in developing nations and affects young adults. The majority of death occurring due to TB are also in the developing world. Overall, around one-third of the world's population is currently infected with the TB bacillus and 5-10% of people who are infected with TB bacilli shows symptoms of active TB. People having HIV and TB infection both are more prone to develop active TB. The risk for developing TB disease is also higher in persons having diabetes, other debilitating disease leading to immune-compromise, poor living conditions, tobacco smokers etc.

After the discovery of rifampicin and isoniazid, tuberculosis has become treatable with a complete course of antibiotics. However, due to the complex nature and long duration of drug treatment, drug abuse has endangered the present first line of drugs. *Mycobacterium tuberculosis* have started to develop resistance against many of these drugs and threatened the whole TB control programs in many developing countries, as treatment is longer and requires more expensive drugs. If resistance to the two most effective first-line TB drugs i.e.

Rifampicin and isoniazid have developed then that kind of tuberculosis is defined as MDR TB. Extensively drug-resistant TB (XDR-TB) is the one which there is resistant to three or more of the six classes of second-line drugs (Control and Prevention 2006). To combat TB, clinical trials were done in the 1970s by Tuberculosis Research Centre, Chennai, India and that resulted in Directly Observed Treatment Short course (DOTS) strategy of tuberculosis treatment which is currently endorsed by recommended by WHO (Farmer 2001). In 1993, The World Health Organization (WHO) declared TB a global health emergency and the Stop TB Partnership has developed a Global Plan to Stop Tuberculosis. It aims to save 14 million lives between 2006 and 2015 (WHO 2006) (Figure 3).

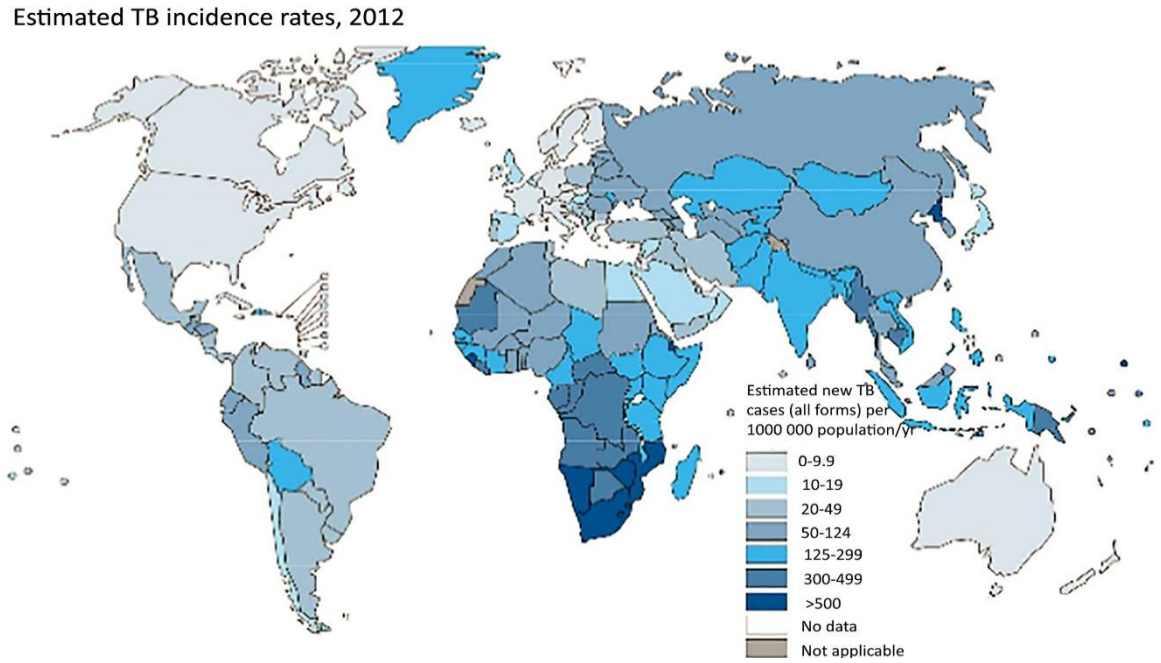

Figure 3: High Burden Countries according to WHO data

3.1 Multi-drug-resistant tuberculosis (MDR-TB) and extensively drug-resistant tuberculosis (XDR-TB)

MDR-TB is multi drug resistant tuberculosis, which develops when the Mycobacterium strains become resistant to either INH or RIF drug (Espinal 2003). Globally, the emergence of Multi drug resistant TB (MDR-TB) and extensively Drug resistant TB is a major threat to TB Control. Resistance to anti-TB drugs in populations is a phenomenon that occurs primarily due to poorly managed TB care such as inconsistent or partial treatment. In such cases, patients do not take all their medicines regularly for the required period because they start to feel better, or doctors and health workers prescribe the wrong treatment regimens, or because the drug supply is unreliable or erratic (Farmer 2001). MDR-TB takes the same route of infection as drug-sensitive TB and in the same manner and is spread readily (Wood and Iseman 1993). Resistance to the first and second line drugs causes MDR-TB. MDR-TB are treated with second-line drugs i.e., Amikacin, Kanamycin, or Capreomycin. When bacteria start showing resistance to most of the first and second line of drugs then this

condition is termed as XDR-TB (Raviglione and Smith 2007). The main cause of the disease is the misuse of the drugs by MDR-TB patients.

There were an estimated 450 000 cases who developed multi-drug resistant TB (MDR-TB) till 2012. The true data of XDR-TB is not known as many countries don't possess the necessary equipment and capacity to diagnose it. It is estimated that there are around 40,000 cases per year. By 2013, 84 countries have confirmed the presence of XDR_TB (WHO 2013). (Figure 4)

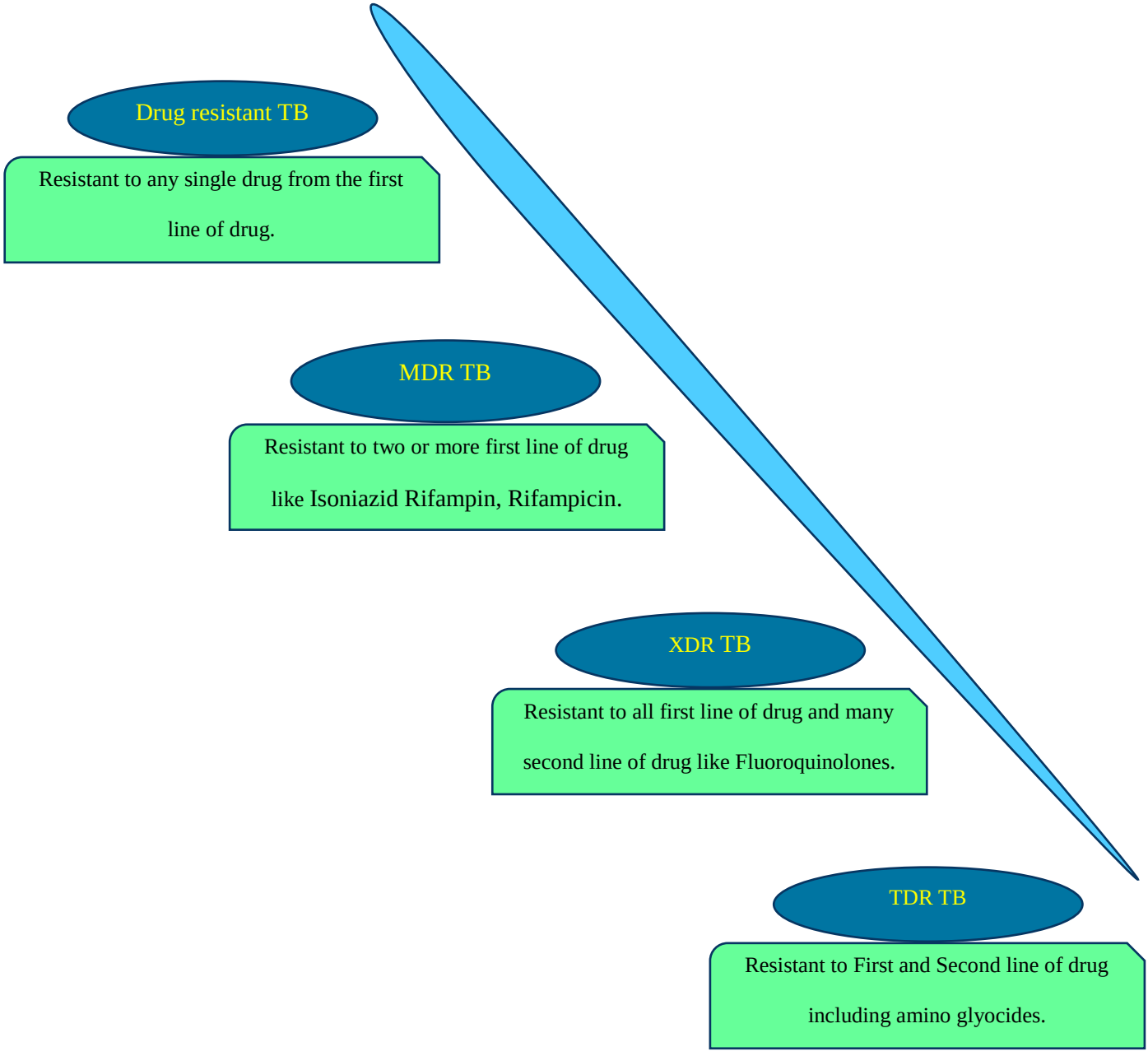

Figure 4: Classification of tuberculosis on the basis of resistance

3.2 The mechanism causing Quinolone resistance in *M. tuberculosis*.

3.2.1 Resistance conferred due to Genetic mutation

Genetic mutation has been considered the fountainhead of evolution as mutation which make the species fitter in the environment and are more suitable for living are selected by nature. This law also guide the evolution of *M. tuberculosis* and confers it drug resistance properties. Due to more survival chances in the presence of antibiotics, the population of resistant strains has been growing at an alarming speed. With the increase in the spectrum of antibiotics, these antibiotics are not only killing the susceptible strains, but also selecting the resistant strains which are resistant to these drugs. In light of this information, numerous current TB medications may well speak to this twofold edged sword.

To understand the exact molecular mechanism of resistance caused by many Quinolone resistant strains of *M. tuberculosis* a functional, biophysical and structural study was conducted by Piton *et al* in 2010. For the first time, Crystallization of both DNA gyrA (GA57BK) and Gyr (TopBK) B subunit was done to perform multiple studies, like X-ray crystallographic studies, sedimentation velocity experiments and activity assays.

- It was confirmed that both subunits together form the catalytic site. Tyr 129 was also discovered to be the catalytic residue which causes cleavage by attacking a phosphate group of DNA and Arg128 involved in resealing the strand.
- During the functioning of an enzyme, a ternary complex is formed between the Toprim and the breakage-reunion domains and DNA. Now this complex forms the binding site for Quinolones and the drug inhibits the enzyme by stabilizing the covalent bond formed between the phosphate group of DNA and Tyr129 of protein complex formed during catalysis.
- It was convincingly shown that Mutation in QRDR region like at 90 and 91 mutation are related to intrinsic resistance development. Ala to Val at 90^{th} codon position and Ser to Pro at 91^{st} codon position are located in the minor groove and forms a gate which restricts the quinolone from reaching the binding pocket.
- Also mutation in the Quinolone binding pocket like at 90, 94 position create stearic hindrance and give the enzyme acquired resistance. Size of residue at 94^{th} position is shown to have direct impact on the level of drug resistance.
- Also mutation at 74^{th} position and at 90, 91 position was shown to induce change in N terminal N-loop position by breaking the crystal contacts which were keeping the loop stable. This results in displacing the loop in such a way that it comes in between the Quinolone drugs and binding cavity. (Figure 5).

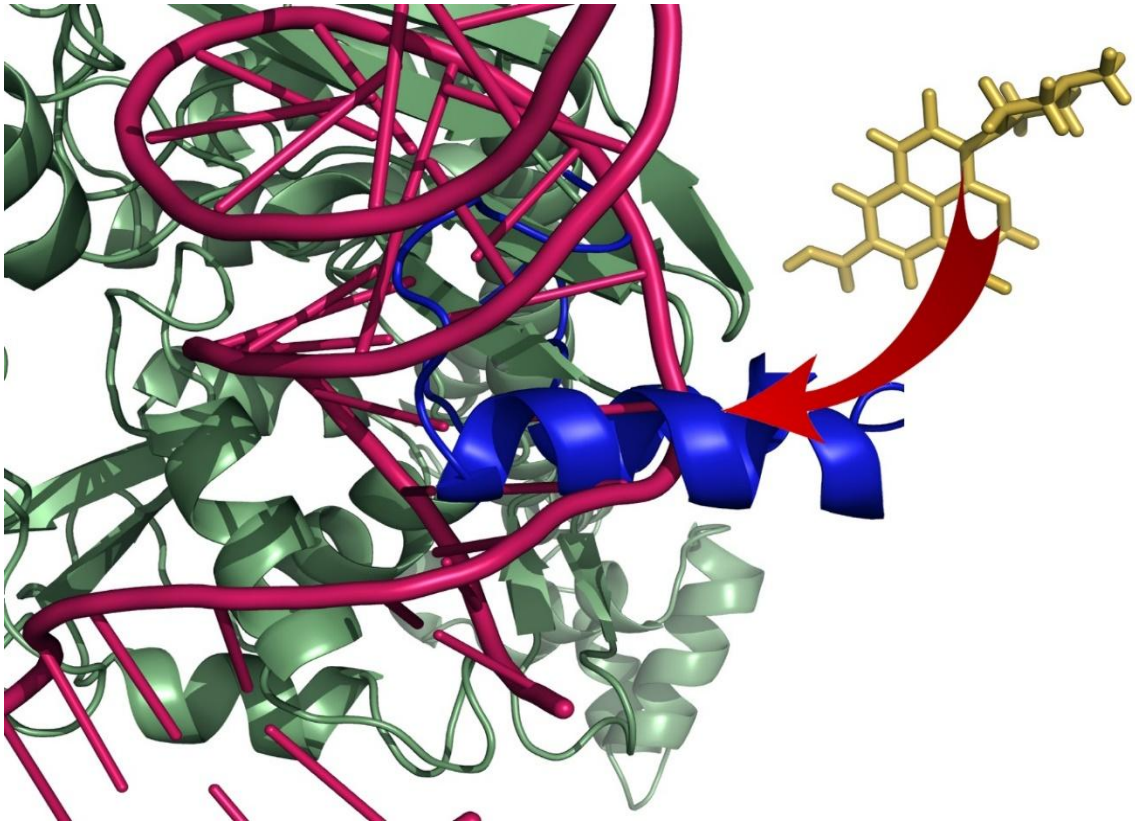

Figure 5: N terminal helix blocking the path of drug by covering the binding site of Ofloxacin.

3.2.2 Resistance conferred due to Molecular mimicry of drug targets

To treat MDR TB, the first drug which is advocated by WHO is a synthetic class of compounds called Fluoroquinolones and it plays a significant role in controlling MDR-TB. However, the emergence of resistance against Fluoroquinolones has made the situation extremely challenging as it has threatened to increase the number of XDR TB or TDR TB.

Apart from mutations induced resistance, one protein namely MfpA has been identified which confer resistance to Fluoroquinolones in *M. smegmatis* (MfpA). A study conducted by Montero *et* al in 2001 proposed this mechanism in Mycobacterium. Overexpression of mfpA results in enhanced resistance to ciprofloxacin and sparfloxacin in *M. smegmatis* and *M. bovis* (Montero, Mateu et al. 2001) and deletion of mfpA leads to decreased Fluoroquinolone resistance. This indicates that the resistance level depends on mfpA expression and varies accordingly.

Based on Montero's study, another study conducted by Hegde *et al in 2005*, proposed a novel mechanism for Fluoroquinolones resistance in *Mycobacterium tuberculosis*. It has been proposed that MfpA like protein is also present in *M. tuberculosis*. It mimics DNA structure and presents a binding site similar to binding site presented by Gyrase-DNA complex. This protein, thus shows similar affinity to the drug and captures the Fluoroquinolones in the cytoplasm, thus saving DNA from the drug attack (Hegde, Vetting et al. 2005).

3.2.3 Mutation inducing resistance against Quinolones class of drugs.

Mutation responsible for resistance against Fluoroquinolones in *M. tuberculosis* were identified and characterized by Alangaden. They amplified QRDR region of a susceptible strain, H37Rv and the resistant mutant strain A382 and A564 strain. They compared it with the nucleotide sequence of the Fluoroquinolone resistant strain. Two single point mutations were detected in this study, first was the substitution of Asp at 87th position by Asn and second was the substitution of Ala at 83rd position by Val (Alangaden, Manavathu et al. 1995).

In 1996, a similar study by XU et al, in 1996 he examined 13 isolates by sequencing the DNA gyrase A nucleotide sequence. 5 isolates having resistant to ciprofloxacin were identified. (Xu, Kreiswirth et al. 1996). At 90th codon position substitution of Ala by Val was seen. At 94th position four different types of substitution that is substitution of Asp by His, Asp by Asn, Asp by Tyr and Asp by Gly were reported in this study.

In 2004, 138 clinical isolates of *M. tuberculosis* were examined by Cheng et al. To detect mutation a new strategy was named multiplex PCR amplimer conformation (MPAC) was developed. Genetic proofing of all the isolates were done by MPAC and mutation detected were verified by nucleotide sequencing. 32 isolates showed cross resistance to multiple drugs of Quinolones class. The mutations were mainly found to be located at 90, 91, and at 94 position. At 90th position Ala to Val, at 91st position Ser to Pro substitution were reported. However, 94 position was seen being predominantly mutated as 23 out of 32 isolates had mutation at 94 positions, Asp to Gly, Asp to His, Asp to Asn, Asp to Tyr and Asp to Ala substitution were seen 94th position.

Double mutation conferring resistance was never considered a big threat as it was not normally seen in clinical samples. Shi et al in 2006 reported for the first time, the presence of double mutant conferring Fluoroquinolone (Ofloxacin) resistance at high frequency in clinical samples. 109 samples were studied, among that 87 samples were found to be Ofloxacin resistant and 22 were susceptible to the drug. QRDR region was amplified by using PCR technologies. On sequencing the QRDR region of DNA, it was revealed that mutations are predominantly occurring at specific positions of gyrA i.e at codons 90, 91, and 94 and at 94 position four different types of point mutations are occurring (94Asp to Gly, 94Asp to Ala, 94Asp to Tyr and 94Asp to Asn), at 90th cordon Ala to Val mutation and at 91st cordon Ser to Pro mutation was observed. This study mostly confirmed the findings of other researchers (Alangaden, Manavathu et al. 1995, Xu, Kreiswirth et al. 1996, Cheng, Yew et al. 2004). Also a natural Polymorphism which has been observed by others at codon position 95 was also seen in all the 109 clinical isolates, it has been found that this natural mutation has no effect on Fluoroquinolone's binding affinity to DNA gyrase.

However, two unique observations were made and reported for the first time.

- First observation was made that 49 isolates of the 87 Ofloxacin-resistant isolates (56%) had double point mutations.

- Second was that a unique Ala74Ser mutation in 20% (10/49) isolates was reported among these double-mutated isolates, this mutation has not been reported earlier in DNA gyrase enzyme.

Discovery of Double point mutation in DNA gyrA was thought to be relatively rare and is not expected to be observed frequently in clinical isolates. So, the high rate at which these double point mutations were observed in gyrA and Ala74Ser mutation shows the development of Fluoroquinolone resistance after prolonged Fluoroquinolone exposure. A real threat of development of extensively drug-resistant (XDR) strains has been posed by the findings of this study (Shi, Zhang et al. 2006).

Drug resistance conferring mutations are normally found to be present in only two short distinct sections of the DNA gyrase enzyme sequence and is termed as the Fluoroquinolone resistance-determining regions (QRDR). This QRDR segment is located in the breakage-reunion domain of GyrA subunit (QRDR-A) and sometimes has been seen in the Toprim domain of GyrB (QRDR-B) but the frequency of mutation occurring in Gyr B is very less (Figure: 6) (Aubry, Veziris et al. 2006, Veziris, Martin et al. 2007). As per WHO 2013 report, What makes this resistance to Fluoroquinolone a very serious condition is that 32.0% of all people suffering from MDR-TB have developed resistance to Fluoroquinolone drug and now are classified as patients with XDR TB (WHO 2013).

3.3 Why target DNA Gyrase?

In case of MDR-TB, WHO advocates Fluoroquinolone drugs like Ofloxacin have been advocated by WHO when predisposition to the first line drug's report are not available in the continuation period (18 months) before changing the course of treatment or if resistance to at least two drugs rifampicin and isoniazid is proven (Walwaikar, Morye et al. 2003). Two type II topoisomerases enzyme that is DNA Gyrase and Topoisomerase IV are targeted by Fluoroquinolone drugs. Apart from killing active and disease causing *M. tuberculosis* another Advantage of targeting type II topoisomerases enzyme is that these Fluoroquinolone also have a bactericidal effect against non-replicating mycobacteria and this might help in reducing the duration of TB therapy. Key for controlling both wild type and multi drug resistant type TB is the search of a novel inhibitor of *M. tuberculosis* DNA gyrase which makes it effective against both.

Type II topoisomerases are crucial enzymes in involved in the controlling and modifying DNA topology and more importantly, it also regulates the supercoiling of DNA (Champoux 2001). ATP dependant Type II topoisomerases induces break in double-stranded DNA (Champoux 2001). DNA gyrase and topoisomerase IV are Type II topoisomerases and both of them are usually coded by the bacterial genome. DNA gyrase aids in relaxing of DNA at the replication forks by inducing a nick and DNA topoisomerase IV is very specific in function, it mediates in the unlinking of interlocked daughter chromosomes (Levine, Hiasa et al. 1998). However the tuberculosis causing agent *Mycobacterium tuberculosis* have only one

type of type DNA II topoisomerase enzyme and that is DNA gyrase (Cole, Brosch et al. 1998). So it performs both the functions, like other DNA gyrase it efficiently supercoils DNA and along with that it also performs the function like inducing breaks in DNA, relieving the tension in DNA strands supercoil and after DNA replication unlinking of daughter DNA (Aubry, Mark Fisher et al. 2006). Both Type II topoisomerases are comprised of two subunits of GyrA and GyrB each and together they form the catalytically active heterotetrameric enzyme (i.e. A2B2). Subunit A consists of two domains, the N-terminal breakage-reunion domain which is from residue number 9 to 501and a C-terminal domain (CTD) encompasses from 512 to 838. ATPase domain extending from 1 to 448 residues, followed by the Toprim domain extending from 448 to 654 residue position makes the subunit B (Figure 6) (Schoeffler and Berger 2008). The function of the breakage - reunion domain also known as G segment at the DNA gate is to bind the DNA segment, cleave and reseal it. On the binding of ATP with N-terminal ATPase domains it undergoes dimerization and then it holds the DNA strand known as a T - segment. This segment is then moved through the nick created in the G-segment by the breakage-reunion domains. Then breakage-reunion domains again reseal and release DNA and T segment is freed through the C Gate and the enzyme regains its open clamp form. Fluoroquinolone shows its powerful bactericidal activity by meddling with the enzymatic reaction process of bacterial type II topoisomerases. Binding affinity to the enzyme type II topoisomerases is quite low but to the enzyme-DNA complex it is very high. It binds and stabilizes the covalent bond formed between 129 Tyrosine residue of enzyme and DNA phosphate. Stabilization of this ternary complex hinders with normal function of the enzyme and halts the DNA replication process which ultimately causes bacterial cell death (Oates, Wood et al. 1991).

Since this enzyme performs an essential function for the survival of *M. tuberculosis* and have only 19% similarity to the human enzyme. So, it has the qualities of a good target for killing the tuberculosis bacteria. Also, it has been successfully targeted for a long time and drug targeting this enzyme like Quinolone are available commercially. These drug's success in inhibiting the bacteria have shown the DNA gyrase's worth as a target. So we have chosen Mtb DNA gyrase as a target for our study.

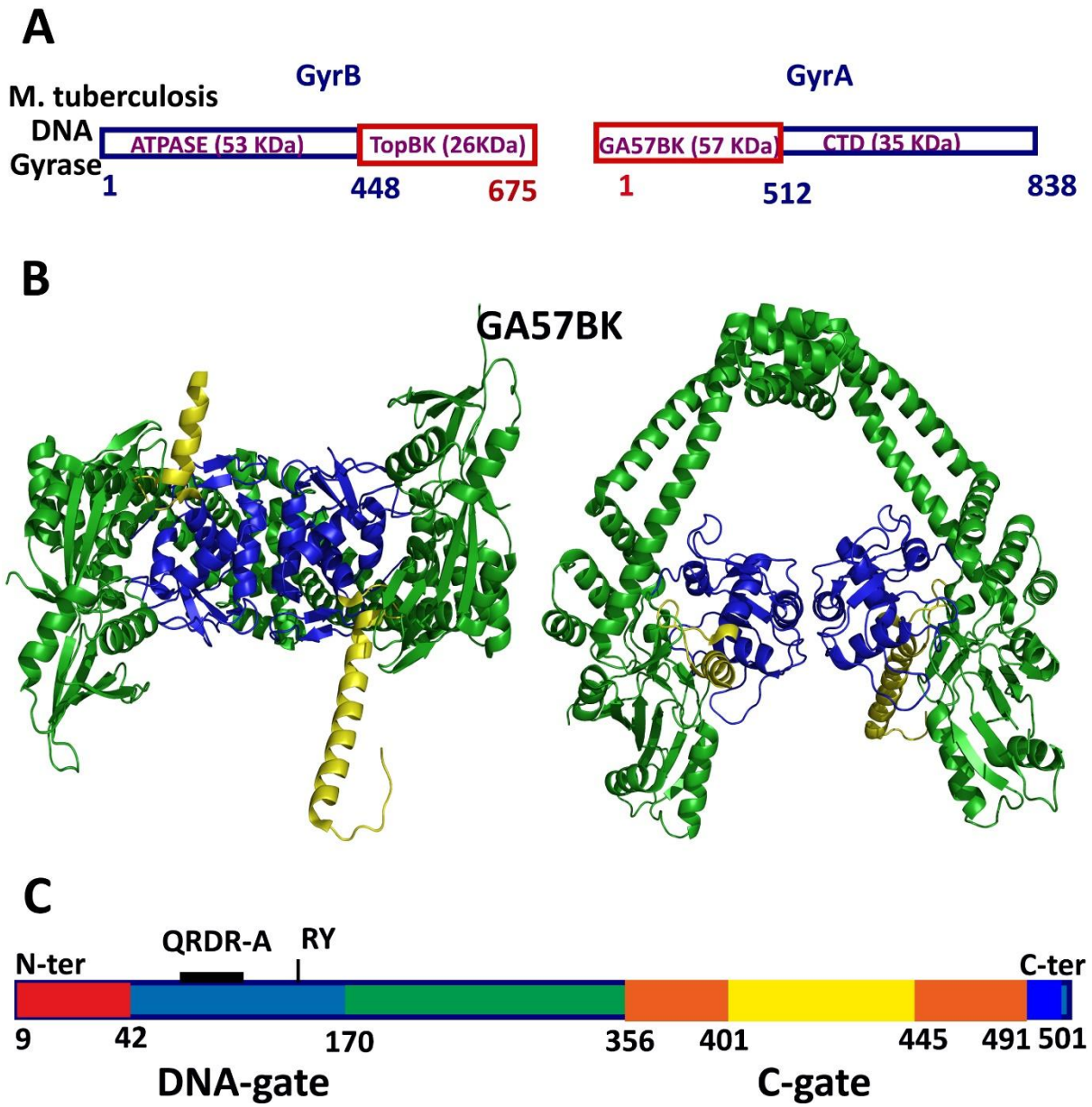

Figure 6: Domain organization and structures of the individual domains from the *M. tuberculosis* DNA gyrase catalytic core. (A). Domain organization of the *M. tuberculosis* DNA gyrase. (B) Two views of the dimeric breakage-reunion domain from *M. tuberculosis* colored by regions. The crystal structure of the complete breakage-reunion domain (GA57BK) extends from D9 to A501. The N-terminal helix is colored with Yellow, the DNA-gate containing the catalytic residues R128 and Y129 and the QRDR-A in blue, rest protein in green. (C) Domain organization of breakage-reunion domain (GA57BK)

3.4 HTVS as means of new drug candidate identification

Despite of having a number of potent drugs for tuberculosis, hunt for new potential drug candidates are going on because of decrease in effect of drug due to the development of drug resistance. Here the need arises for a fast and reliable technique to screen a huge number of chemical products available to explore their potential therapeutic activities to cut down on the

time and cost involved in the *in vivo* identification of drugs. Virtual Screening is a computational methodology used to speed up the drug discovery, it is employed to enhance and complement High Throughput Screening (HTS) for hit recognition.

Structure-based discovery of antibacterial drugs using Virtual Screening

1990-70 was the era of drug discovery in which almost all the presently available drug were discovered. However the development of bacterial resistance has forced us to keep discovering or designing more novel drugs. Availability of Bacterial genome and development of proteomics led huge data assembly, till date total over 90 000 crystal structures of protein have been deposited in the PDB database. High throughput screening has given promising results in the field of cancer, asthma, diabetes. Taking its success into account, it can also be employed in search of next generation antibacterial drug.

Structure based drug discovery (SBDD) most successful example can be seen its application in HIV/AIDS, in which crystal structure of HIV protease lead to identification of its five inhibitor. Robert *et al* in 1990 prepared a series of peptides. These peptides were based on the transition state mimitcs concept. Once the series was formed, using various computational technique a common inhibitor of HIV1 and HIV2 was identified. ADMET properties were also studied and Amprenavir was identified as the most potent inhibitory agent. Their cytotoxicity was also found to be least among all as no cytotoxicity was detected at 10 and 5 mM. Amprenavir was found to inhibit HIV protease by inhibiting the cleavage of p55 to the viral protein p24. The success of Amprenavir as a drug boosted the SBDD methodology of drug discovery (Roberts, Martin et al. 1990).

Drugs like Nelfinavir and Viracept was identified by Kaldor *et al* in 1997, it was also produced from the structure based lead identification approach. It is a nonpeditic inhibitor HIV-1 protease. *In vivo* studies were also performed on these drugs. These studies proved that it is absorbed quite well in oral mode and have favourable pharmacokinetic properties in humans. (Kaldor, Kalish et al. 1997). Also, the drug Zanamivir for influenza (Highleyman 1999) was also developed using SBDD based virtual screening approach.

Principle of SBDD based virtual screening

The principle behind interaction of drug and target protein is molecular recognition. The rational drug design requires a molecular understanding of how the drug will interact with its target in terms of structure and energetics. Structural information can be gained by X-ray crystallography or NMR but if no crystal structure is available, one can go for the homology modelling to get the 3D structure. Next step is to identify the residue forming active sites, these residues are then selected for grid formation where small drug molecules are docked. Screening of lakhs of compounds needs a computationally cheap estimate of binding energy represented by docking score. This is achieved by using scoring schemes that involve different force fields to measure the interaction in terms of energy and empirical and knowledge based methods (Villoutreix, Renault et al. 2007, Halgren 2009).

Lately SBDD programs were based on a single high resolution protein crystal structure. However, since a crystal structure is like a snapshot of protein in one form at a particular instance, it presents a problem while designing the ligands, as biologically active form may be conformationally different to the crystal form. There are two methods to counter it, one is to let the crystal structure undergo simulation till the structure is stable. Second is to perform flexible docking and best is to perform both. But flexible docking and simulation drastically raises the computational time. So overcome the problem, High throughput screening serves a link in the chain comprising the industrialized drug discovery paradigm. This protocol first screen the compound by estimating the binding energy. This scoring is not very accurate but is very fast. Then the selected compounds are docked again using flexible docking. This way hits are selected which have significantly higher chances of success (Carlson and McCammon 2000, Jain 2007).The growing burden due to drug resistance has created the need for fast, efficient and effective techniques for drug discovery and HTVS can play a big role.

3.5 Significance of Phytocompounds in drug discovery

Traditionally, natural products have been the main source of novel lead molecule in the drug discovery process. But in early 2000, most of the pharma companies have either terminated or scaled down their natural production operations. Decoding the human genome and development of technologies like combinatorial library Reason for downfall. A company focused on combinatorial library as it was capable of generating millions of synthetic compounds, which would then be screened by high throughput screening technique. Handful of promising lead compound resulting from HTS would be purely synthetic compound and will pose not patent threats which are usually involved with natural products. But the promising technologies didn't gave the desired result and serious doubts were raised about their usefulness.

Lipinski was quoted on combinatorial library that "The combinatorial libraries in the early years were so flawed that if you took the libraries across the Pharma from 1992 to 1997 and stored them in dumpsters you would have improved productivity". However, apart from quality of library another reason for let-down was that the proposed synthetic inhibitors fail to clear preclinical or clinical trial due to drug related or drug induced toxicities and also due to different chemical space occupied by synthetic compounds as compared to natural product (Arya, Joseph et al. 2002, Burke, Berger et al. 2003).

Slowly, interest in natural product has started to rise steadily. The need arises for finding natural products or their derivatives having the potential to act as inhibitors against the cancer molecular targets, anti-infective, immunosuppression and antimicrobial agents have increased due application of same HTVS technique which was earlier used on synthetic library. Most of the phytocompounds do follow the Lipinski's rule of five. Even the phytocompound with high molecular weight, rotatable bonds and more stereogenic centers retain relatively low Log P values. Thus, these have a high tendency to get absorbed more easily as compared to the conventional synthetic drugs. With the availability of number of chiral centers (Feher and

Schmidt 2003) along with a wider distribution of molecular attributes like octanol-water partition coefficient, molecular mass and diversity of ring system, make natural products more suitable to be used as drugs (Lee and Schneider 2001).

In a study by Lipinski, Lipinski rule of 5 (Ro5) for predicting effective oral absorption or permeation was proposed. It was reported that a good lead compound should have less than 5 H-bond donors, 10 H-bond acceptors, the molecular weight (MWT) should be less than 500 and the calculated Log P (CLogP) should be less than 5 (or MlogP > 4.15). Lipinski stated that the Rule of 5 is derived from a study of biochemical and physical features of 1000's of drugs. He reported that a portion of dataset didn't comply with his rule of 5 and most of them are effective drugs. Interestingly, those therapeutic drugs which were falling outside the rule of 5 were mostly natural products. Those orally active drugs belonged to different therapeutic classes like antibiotics, antifungals, vitamins and cardiac glycosides. Reason for this odd behaviour of natural products was explained by saying that these classes possess structural features that allow the drug to behave as a substrate for naturally occurring transporters. Thus, application of the Lipinski rule of 5 for predicting do not hold much importance in natural compounds (Lipinski, Lombardo et al. 2012).

3.6 Application of High Throughput Screening Leading To Hit Identification.

This study, conducted by park et al in 2012, has reported identification of inhibitor of the breakpoint cluster region-Abelson tyrosine kinase. This enzyme is known to be responsible for chronic myelogenous leukemia. Imatinib is the FDA approved drug which has been used for treating the disease (Capdeville, Buchdunger et al. 2002). However, with time, resistance to this drug has been noticed due to mutations in the kinase domain of the breakpoint cluster region-Abelson enzyme (BCR-ABL). Around 100 point mutations have been detected in the Imatinib resistant chronic myelogenous leukemia (CML) patients (O'Hare, Eide et al. 2007). This led to research in developing second generation of drug and some effective drug countering the resistance have produced. Such drug includes Dasatinib, Nilotinib, Bafetib. These drugs managed to control the Imatinib resistant CML to some extent, but resistant caused to T315I mutation proved hard to be managed.

Various drug against wild or mutant CML have been proposed but this study chose a broader goal. They proposed a common inhibitor of wild type and T315I mutant BCE-ABL using Parallel Structure Based High Throughput Virtual Screening (HTVS). Followed by a simulation study to study the stability and binding mechanism of the enzyme. The biggest disadvantage of HTVS is the inaccuracy in the scoring. This leads to poor correlation between computational and experimental results (Warren, Andrews et al. 2006). This study was performed using accurate solvation model for calculating the free energy between ligand and BCR-ABL enzyme. New solvation model for a compound was used to improve the empirical Autodock scoring function. The modified energy scoring function was.

$$\Delta G_{bind}^{aq} = W_{vdW} \sum_{i=1} \sum_{j=1} \left(\frac{A_{ij}}{r_{ij}^{12}} - \frac{B_{ij}}{r_{ij}^{6}} \right) + W_{hbond} \sum_{i=1} \sum_{j=1} E(t). \times \left(\frac{C_{ij}}{r_{ij}^{12}} - \frac{D_{ij}}{r_{ij}^{10}} \right) + W_{elec} \sum_{i=1} \sum_{j=1} \frac{q_i q_j}{\varepsilon(r_{ij}) r_{ij}} + W_{tor} N_{tor} + W_{sol} \sum_{i=1} S_i \left(Occ_i^{\max} - \sum_{j>i} V_j e^{-\frac{r_{ij}^2}{2\sigma^2}} \right),$$

Where, $W_{vd}W$, $W_h$bond, W_{elec}, W_{tor}, and W_{sol} are van der Waals, hydrogen bond, electrostatic interactions, torsional term, and desolvation energy of an inhibitor, respectively. Rig represents the interatomic distance, and A_{ij}, B_{ij}, C_{ij}, and D_{ij} relate to the depths of the potential energy well and the equilibrium separations between the two atoms. The hydrogen bond term has an additional weighting factor, E(t), representing the angle dependent directionality. To obtain the dielectric constant which is important in computing the interatomic electrostatic interactions between BCR-ABL and a ligand molecule cubic equation approach was applied (Park and Jeon 2007). Two common inhibitor of wild and mutant type tyrosine kinase enzyme was identified after HTVS and simulation. In a simulation study, inhibitor showed different binding mode, on probing further it was reported that by acquiring different binding mode, ligand in mutant enzyme is increasing hydrophobic interaction and compensating the loss of H-bonds. Since these inhibitors possessed desired physiochemical properties, they are now reported to have been under study for their SAR studies to optimize their inhibitory activity (Park, Hong et al. 2012).

HTVS has not yet been used as technique for drug discovery in Tuberculosis disease, however Spec et al used QSAR and virtual screening of a relatively smaller set of dataset consisting of only 1054 compounds in search for hit fragments having the property to target multiple enzymes or chain of reaction to have anti-tuberculosis effect. Fragment based Mt-QSAR model was developed using 790 compounds as training set and 264 compounds as a test set. The model was statistically sound and it was reflected in the accuracy with which it tested both training and test set, i.e. with 90% accuracy. After QSAR model generation, the contribution of all the fragment present in the 1054 molecule was evaluated and were screened for inhibitory activity against 6 tuberculosis protein. 5 common fragments were obtained which showed high activity against all the tuberculosis protein. Now by using these 5 fragment 6 new compounds were designed. When these compounds were evaluated by QSAR model, then it showed 100% inhibitory activity against all the six proteins which were being targeted. This study presented another approach along with HTVS as a model for drug discovery ***(Speck-Planche, V Kleandrova et al. 2012)***.

In this study Sharma et al in 2012, targeted L-Aspartate a-decarboxylase (ADC) of *Mycobacterium tuberculosis.* This enzyme is considered critical for *Mycobacterium tuberculosis* as it mediates formation of 4-phosphopantetheine prosthetic group which is required for biosynthesis of fatty acid. It is required by several bacteria including *Mycobacterium tuberculosis* and thus it was treated as a potential target. Methodology

included were protein structure preparation, HTVS of 333, 761 compounds, it was followed by lipinsky screening and then Extra precision Glide docking protocol was used for docking. This study resulted in 8 compounds which showed high potential for inhibiting ADC enzyme. ADMET properties of hose compounds were further studied using Qikprop. To avoid any potential side effect, cross reactivity of lead molecules with SAM decarboxylase was also examined. As this was the only enzyme which shows high structural and functional similarity. Only those compounds were retained which showed very less or no cross reactivity as a lead compounds. A very similar methodology is adopted in the work presented here (SHARMA 2012).

One of the many characteristics of the cell wall of *Mycobacterium* is high content of diaminopimelic acid (DAP). Various gene knockout studies have suggested that DAP pathway is very essential for bacteria and inhibition of this pathway leads to the cell wall lysis. Also, this many enzymes participating in this pathway are absent in humans, so this pathway has become an area of research as inhibiting this pathway would have fatal effects on TB bacteria. Garg et al has taken this pathway as a target for drug discovery. Dihydrodipicolinate synthase (DHDPS) enzyme is involved in catalysing the first step of this pathway and results in meso-DAP formation by condensation of pyruvate with active site residue (LYS-171), it leads to the formation of a Schiff-base. Many broad spectrum drugs are available commercially which also targets DHDPS but their efficacy varies from species to species of bacteria. This group used different computational method to unearth DHDPS inhibitor (Garg, Tewari et al. 2010).

Using leadgrow module of VlifeMDS, a combinatorial library of pyruvate analogues were generated and Lipinski filter was used to get library of only those compounds which satisfy Rule of 5. 4088 compounds were obtained after applying Lipinski filter and this library was used as a dataset for HTVS using Glide protocol. After that top 500 compounds were used for flexible docking, this resulted in 347 analogues which had score better than pyruvate. Detailed analysis of top 10 compounds was carried out using other computational techniques. This was the first study which looked for lead compound in targeting DAP pathway in *Mycobacteria tuberculosis*. Similarly, there are many other targets which are yet left to be explored and can give an effective drug for a new drug.

Considering the need for common drug effective against both wild type and the three double mutants (1. Ala90Val + Ser91Pro, 2. Ala90Val + ASP94Gly, 3. Ala74Ser + ASP94Gly) Fluoroquinolone resistant Tuberculosis (Piton, Petrella et al. 2010). In this study, using Parallel High Throughput Virtual Screening of 1, 69,109 natural compounds of Zinc database and Myria screening databases, Molecular Docking and Molecular Dynamics study, we have identified Chebulinic acid (CA) (Figure 7) , a natural phytocompound obtained from *Terminalia chebula* as a most potent drug candidate to treat both TB and Fluoroquinolone resistant MDR-TB by inhibiting DNA gyrase A. *Terminalia chebula* is one of the three constituent of triphala (Lu, Chakroborty et al. 2012). Triphala has been used since ages in Indian Ayurvedic discipline for curing many ailments related to the gastrointestinal and cardiovascular systems (Singh, Govindarajan et al. 2008, Pawar, Lahorkar et al. 2009, Baliga 2010). Recently, *in vivo* studies in mice has demonstrated that Triphala constituents can inhibit the growth of stomach cancer, murine thymic lymphoma and human pancreatic cancer, it also has antibacterial properties, but its effect particularly on TB have not been studied much (Malekzadeh, Ehsanifar et al. 2001, Deep, Dhiman et al. 2005, Shi, Sahu et al. 2008, Baliga 2010). The study presented here is an attempt to find natural compound which has the bactericidal properties against wild type *M. tuberculosis* DNA gyrase and which can also be effective against multi-drug resistant (MDR)-TB.

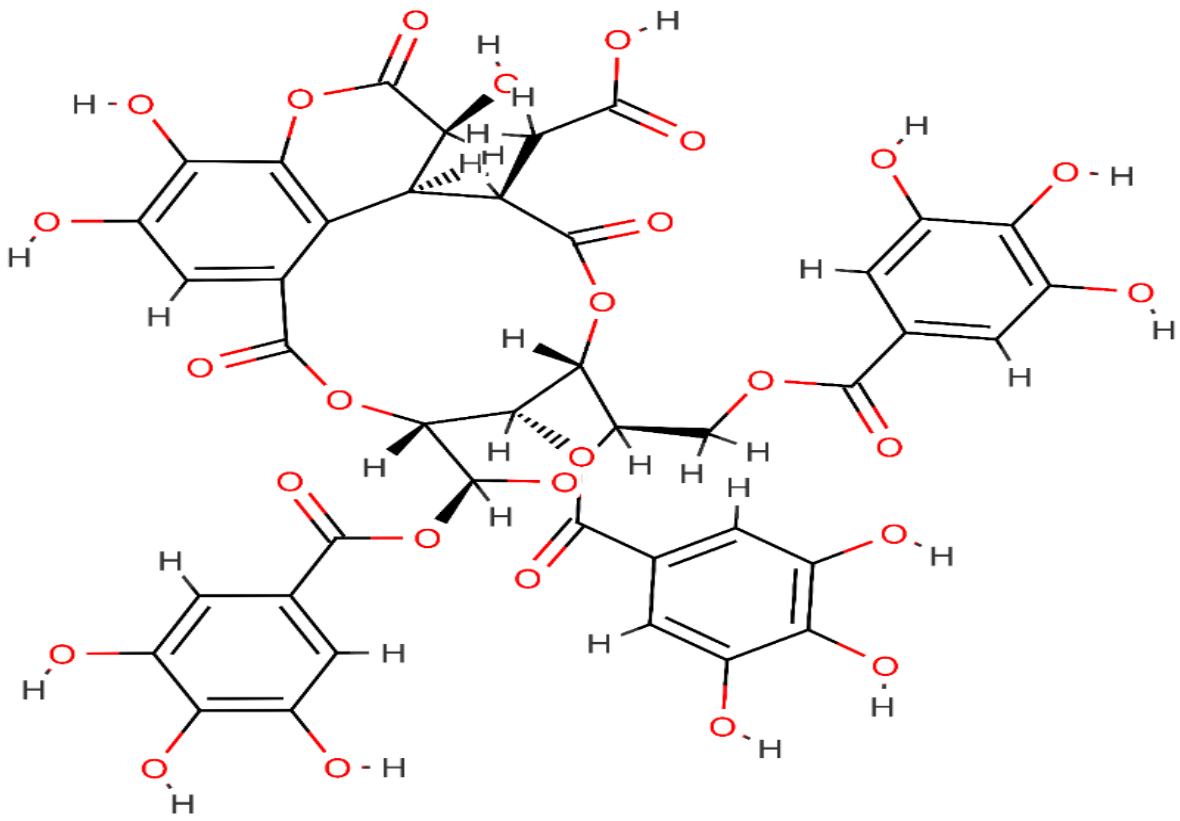

Figure 7: Structure of Chebulinic Acid

4 MATERIALS AND METHODS

4.1 Preparation of wild type and mutated DNA Gyrase A structures

The crystal structure of *Mycobacterium tuberculosis* DNA gyrase A, consisting of two domain i.e. the N-terminal breakage-reunion domain and a C-terminal domain (CTD) having DB access code- 3IFZ and *Streptococcus pneumoniae* topoisomerase IV catalytic core having pdb accession code-3FOF was acquired from Protein Data Bank. Crystal water molecules and all non-bonded heteroatoms including the docked ligand were removed from the protein structure using Accelerys Viewerlite 5.0 (Viewerlite_5.0). For the sake of reducing the computational time only "A" chain of DNA gyrase Subunit A was taken for docking and Molecular Dynamics studies. Using tfmodeller (www.maya.ccg.unam.mx/~tfmodell), DNA was docked with *Mycobacterium tuberculosis* DNA gyrase Subunit A while taking *Streptococcus pneumoniae* topoisomerase IV as a reference sequence (Laponogov, Sohi et al. 2009). *Streptococcus pneumoniae* topoisomerase IV was taken as a reference because the crystal structure of enzyme-DNA complex was available and also it showed maximum sequence identity (41.15) and sequence similarity (62.1%) compared to others. Generated structure was used for analyzing the impact of drug on wild and three double mutant's DNA Gyrase A enzyme structure.

Since the crystal structure of mutant DNA Gyrase A required for HTVS is not available, so three double mutants: were created by incorporating point mutation in the structure. In first double mutant of DNA gyrase A chain A, at 90^{th} position Ala was mutated to Val and at 94^{th} position Asp to Gly. In second double mutant of DNA gyrase A chain A, mutation introduced at 74^{th} position was Ala to Ser and Asp to Gly at 94^{th} position. Similarly, in the third double mutant, at 90^{th} position Ala was mutated to Val and at 91^{st} position Ser to Pro through a protein preparation wizard. The wild type and three mutant DNA gyrase A: 1. Ala90Val + ASP94Gly (90V94G) 2. Ala74Ser + ASP94Gly (74S94G) and 3. Ala90Val + Ser91Pro (90V91P), using Schrodinger's protein preparation wizard all mutant's structure was stabilized through several structural modification and energy minimization (Schrödinger Release 2013-1: Schrödinger Suite 2013 Pro,in Preparation Wizard; Epik version 2.4 , Madhavi Sastry, Adzhigirey et al. 2013). In this process hydrogen atoms were added, bond lengths were augmented, disulphide bonds were generated, capping of terminal residues were done and selenomethionines were converted into methionine. Molecular dynamic simulation was then performed for 12 ns period for all the mutants to get the stable structure which were further used for High throughput screening and docking studies (Figure 8, 9, 10, and 11).

4.2 Binding cavity prediction

In search for a single drug targeting both wild type and mutant type, choice of ligand binding cavity which can produce the desired inhibitory effect is of fundamental importance. Binding cavity was predicted using Q-SiteFinder server (Laurie and Jackson 2005). Q-SiteFinder uses

only energetic criteria to identify binding cavity. This method uses a methyl probe and calculates the van der Waals interaction energies of the probe with the protein. Only those Probes are retained which shows favorable interaction energies and are ranked according to their total interaction energies (Laurie and Jackson 2005). The ranked one cluster was picked as it was more energetically favored for further docking studies.

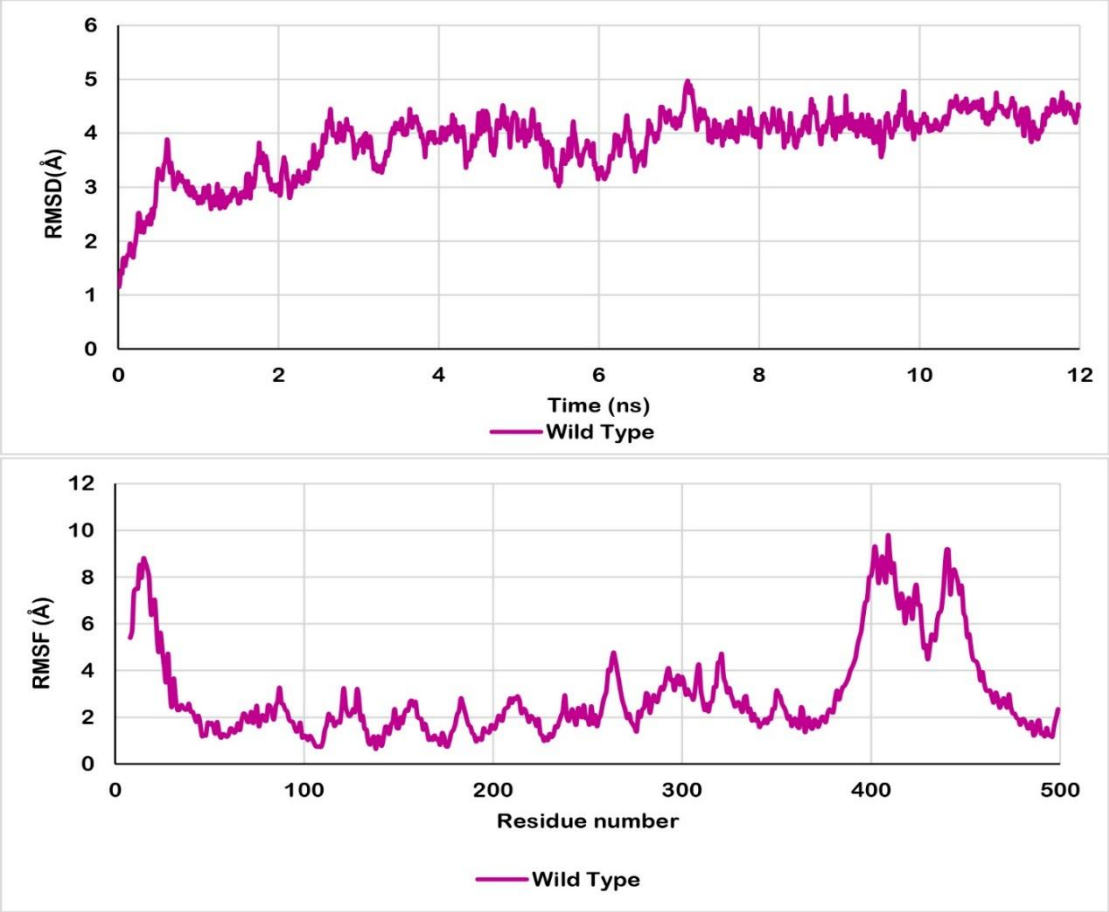

Figure 8: RMSD AND RMSF plot of Wild type DNA gyrA Chain A enzyme after double point mutation, energy minimization and simulation.

4.3 Virtual library preparation for HTVS

To perform HTVS, a data set consisting of 1,69,109 phytocompounds from ZINC database, 190 self-created phytocompound library and also 10, 000 phytocompounds were downloaded from the MyriaScreen database of drug/lead-like compounds in SMILES format (Irwin and Shoichet 2005). By using LigPrep's ligand preparation protocol, the 179 299 compounds were prepared for docking. This protocol generates diverse stereochemical, ionization and tautomeric variants of the 179 299 compounds beside minimization of their energy. After protein and all the compound preparation, the dataset was then used further for virtual screening and docking studies.

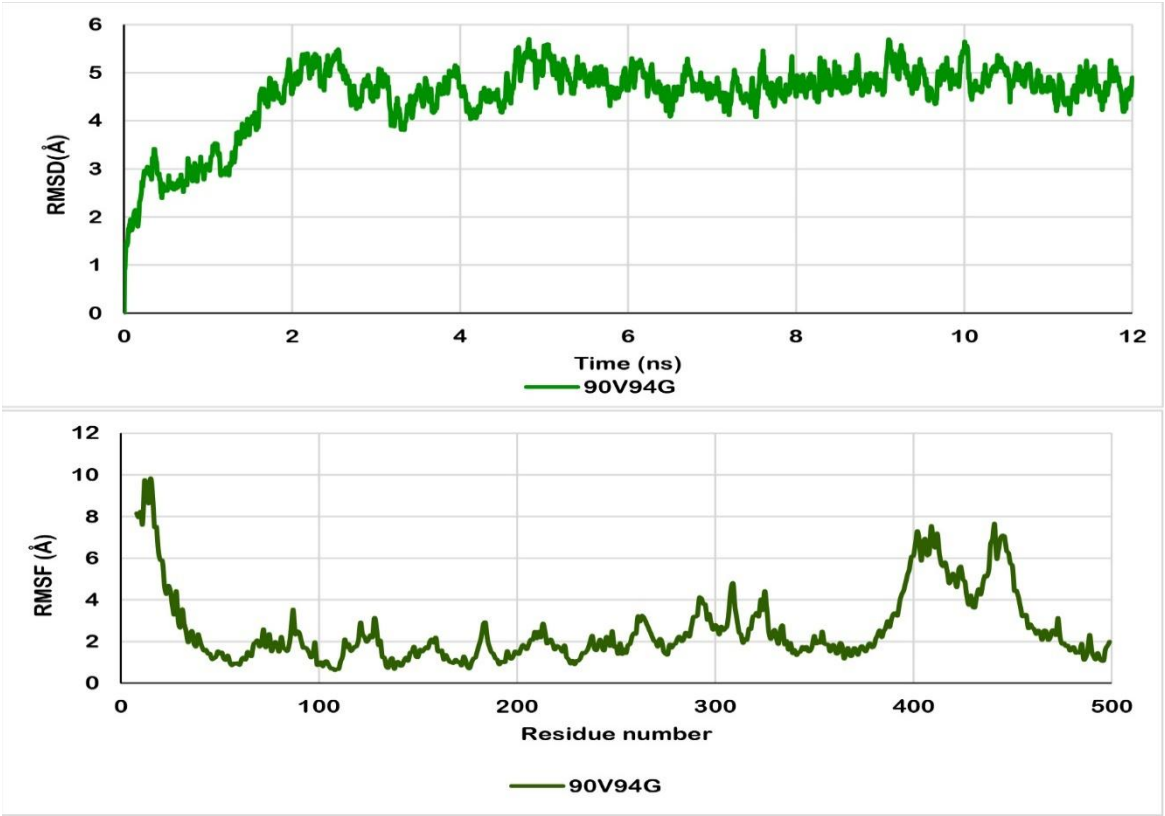

Figure 9: RMSD AND RMSF plot of 90V94G DNA gyrA Chain A enzyme after double point mutation, energy minimization and simulation.

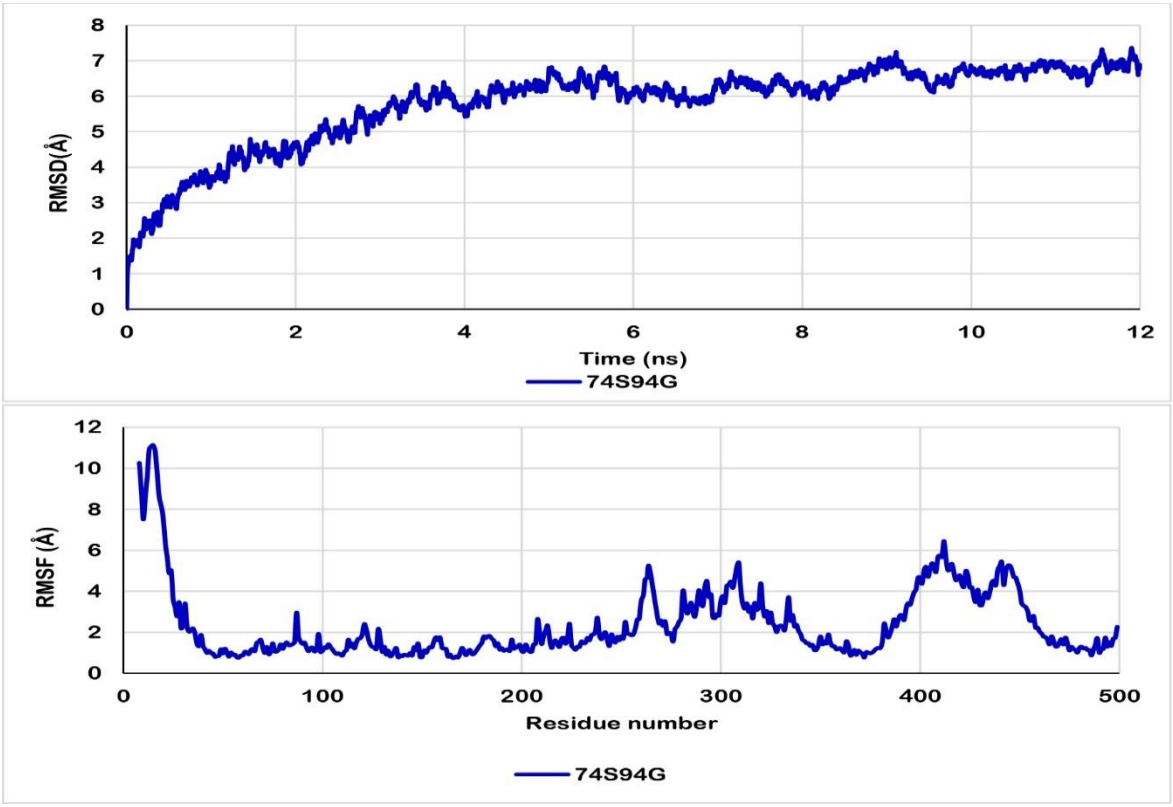

Figure 10: RMSD AND RMSF plot of 74S94G DNA gyrA Chain A, enzyme after double point mutation, energy minimization and simulation.

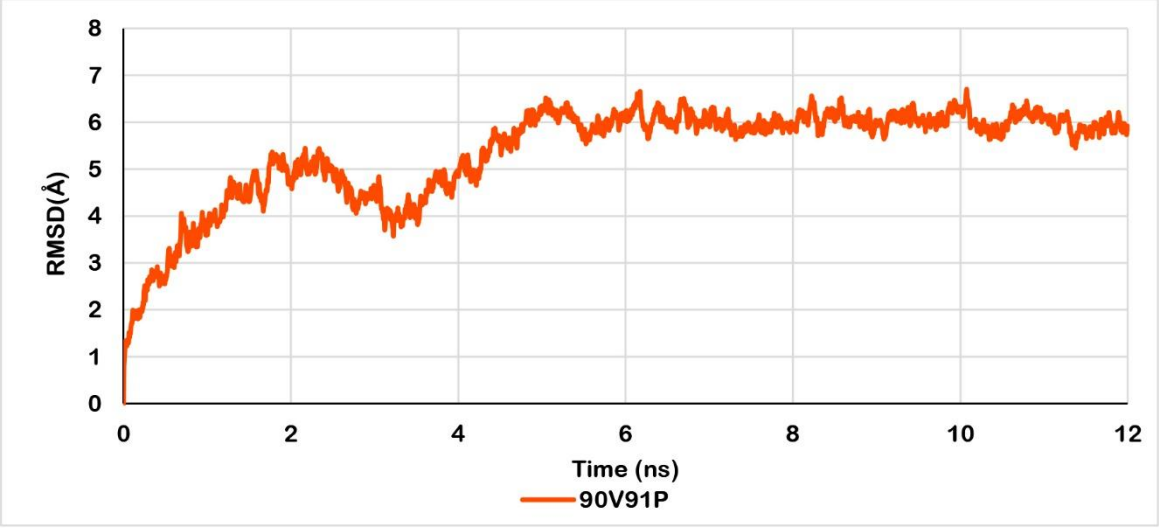

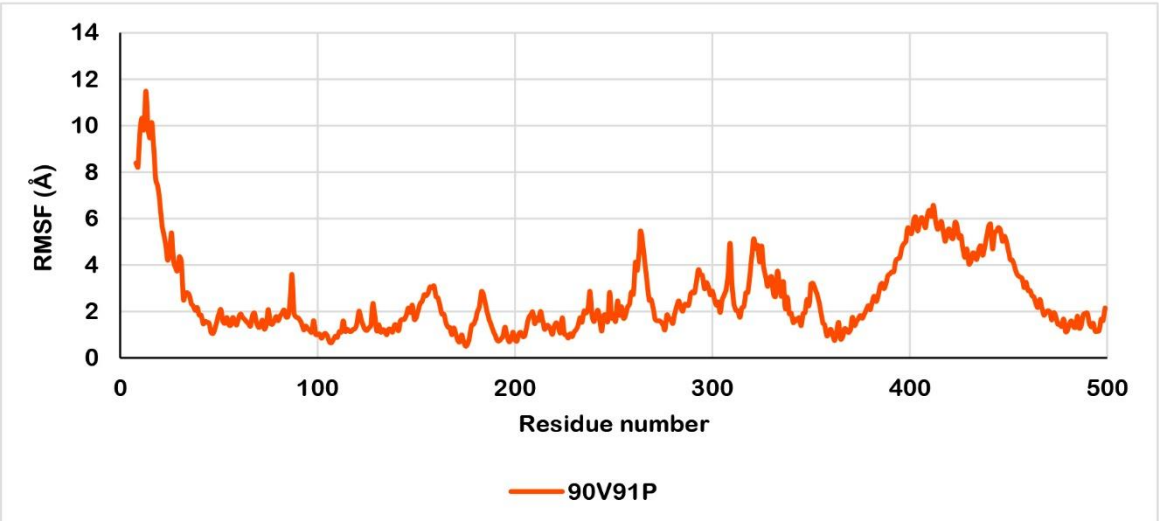

Figure 11: RMSD AND RMSF plot of 90V91P DNA gyrA Chain A enzyme after double point mutation, energy minimization and simulation.

4.4 High throughput virtual screening and docking studies

Glide docking module of Schrödinger was used to create a lattice around the residues present in the binding cavity of prepared DNA Gyrase A chain A structure (Friesner, Banks et al. 2004, Halgren, Murphy et al. 2004). High throughput virtual screening of the dataset was done against the DNA Gyrase A at chosen lattice coordinates employing Glide model's HTVS docking protocols. Those compounds which scored above -5.50 in HTVS docking score were retained and the rest was discarded. Retained compounds were subjected to extra precision docking with same Wild type DNA Gyrase A monomer using Glide's XP protocol for docking score refinement. The same HTVS Glide protocol and XP glide docking protocol were used for screening using the same grid with the selected 1,79,109 compounds against DNA Gyrase A chain A of all the three double mutants: 1. 90V94G 2. 74S94G and 3. 90V91P. HTVS cutoff was kept at -5.5 and XP docking cut off was kept at -6.0 for the screening.

After HTVS and XP docking, the top scoring compounds from wild type screening were compared to the 90V94G's screening result and all the compound which were common in both and having XP docking score above -6.0 against wild type were obtained. The obtained result was then compared with the XP docking result of 74S94G mutant and again compound common to both were retained and the rest was discarded. The retained compounds were then compared with the XP docking result of 90V91P and all the compounds were discarded except the common ones. By this progressive screening, we got a list of compounds which shows good binding affinity for all the four wild and mutant DNA gyrase A at the desired site. Thus, this compound was then inspected through MD simulations to study in detail its dynamic mode of molecular interaction with the respective protein molecules. All docking studies using Glide protocol were completed on i7 processor @ 2.8GHz with 8.00 GB RAM and Schrödinger 9 Maestro interface was compiled and run under Ubuntu 64 bits operating system.

4.5 Molecular dynamics simulations of ligand-bound complexes

To get more insight into protein-ligand complex and its stability, the molecular dynamic study was performed using Desmond Molecular Dynamics module of Schrodinger maestro (Jorgensen, Maxwell et al. 1996) which apply optimized Potentials for Liquid Simulations (OPLS) all-atom force field 2005 (Kaminski, Friesner et al. 2001). Prepared protein-ligand complexes were solvated with TI4P water model in a triclinic periodic boundary box for MD simulations. To prevent the direct interaction of protein complex with its own periodic image a boundary box is created and distance between protein complex and box wall is kept at 10 Å. Steepest descent method was used to minimize the energy of the prepared structures for a maximum of 5000 steps till a threshold of 25 kcal/mol/Å is achieved. After that minimization using Low-memory Broyden quasi-Newtonian minimizer was done until a convergence threshold of 1 kcal/mol/Å was attained. The other parameters were kept as default for system equilibration. MD simulations were for a period of 12-16ns at a constant temperature of 300 K, pressure 1 Atm and at time step of 2 femtoseconds (fs). Smooth particle mesh Ewald method was used for calculation of long range electrostatic interactions (Essmann, Perera et al. 1995) during the MD simulations. Columbic short range interactions were also calculated using a cut-off scheme, with a cut-off radius of 9 Å for calculation. The protein ligand complex was prepared for MD simulations using the above mentioned parameters. MD Simulation was then carried for a time period of 12-15ns.

The root mean square deviation (RMSD) of wild and three mutant type DNA gyrase A chain A was docked with ligand within the binding pocket was calculated for the entire simulation course with the reference to 1st frame. To study the interaction between ligand and protein, ligplot program was used to find hydrophobic interactions and H-bonds formation (Wallace, Laskowski et al. 1995). For H bond formation, maximum distance between acceptor–donor atoms was set as < 3.3 Å and acceptor-H donor angle greater than 90°.

5 RESULTS AND DISCUSSION

5.1 Binding cavity prediction

Q-SiteFinder server predicted 5 binding cavities and are ranked according to their total interaction energies (Laurie and Jackson 2005). The ranked one cluster was picked as it was most energetically favoured for further docking studies. The wild type structure was submitted on the Q-Site server and best predicted cavity included 36 residues namely Leu41, Glu43, Gly47, Leu48, Lys49, His52, Ser95, Leu96, Arg98, Met99, Trp103, Ser104, Leu105, Arg106, Val110, Asp111, Gly112, Pro119, Gly120, Asn172, Asn176, Ser178, Gly179, Ile180, Ala181, Asn188, Ile189, Pro191, Val270, Leu274, Tyr276, Gln 278, Asn279, His280 and Phe341 with cavity area 611 A2 and cavity volume 1100.7A3. The same binding cavity was used for grid generation in all the wild type and double mutant DNA Gyrase A structure for Docking (Table 1).

Cavity	**Wild type**	**90V94G**	**74S94G**	**90V91P**
Volume (Å3)	1100.7	1472.2	1472.3	1443.5
Area (Å2)	611	822.1	824.4	769.8

Table 1: Binding cavity size and area

5.2 High Throughput virtual screening and XP docking studies

In order to identify potent inhibitor against DNA gyrase A, HTVS Glide docking protocol was used to screen 1, 79,299 drugs like compound from the Zinc database and Myria-screening database. After the screening of the compound dataset against the Wild type DNA gyrase A chain A with grid around the binding cavity predicted by the Q site finder, around 5200 compounds were obtained with HTVS docking score above -5.5. All these ligands were then taken as an input dataset for XP docking protocol for Wild type DNA gyrase A chain A using the same grid. XP docking performs more accurate docking and out of thousands of compounds, 2011 compounds were obtained with XP docking score greater than 6.0. Then for identifying potent inhibitor against mutant 90V94G DNA gyrase A, again same HTVS was used to screen the same library and 4236 compounds were obtained with HTVS docking score greater than -5.5. These compounds were then subjected for extra precision docking and 1224 compounds were found to have XP docking score above -6.0 using the same grid for all the mutant. The same HTVS process was repeated for 74S94G DNA Gyrase A chain A and 90V91P and 10183, 134 compound were obtained with HTVS docking score greater than -5.5 respectively.These selected compounds after HTVS were then used for extra precision docking with same grid against both the mutant gyrase enzyme A and 357 compounds were found to have XP docking score above -6.0 for 74S94G DNA Gyrase A and only 31 compounds were found to have XP docking score above -6.0 against 90V91P. XP docking Results of Wild type Gyrase A were compared to 1st mutant 90V94G DNA gyrase A chain A and 122 compounds showed considerable binding affinity with a minimum XP

docking score of -7.0 for 1st double mutant. These 122 compounds were then checked for binding affinity with the 2nd mutant 74S94G DNA Gyrase A chain A and 11 out of 122 compounds with XP docking score ranging from -15.94 to -7.42 showed a favourable binding affinity towards the wild and first two mutants DNA Gyrase A chain A. These eleven compounds were subjected to screening against the third mutant 90V91P DNA Gyrase A chain A and five compounds were found to be showing appreciable binding affinity with docking score ranging from -15.11 to -7.08. Among the five, CA, a natural phytocompound obtained from *Terminalia chebula* show maximum binding affinity and had XP docking score -14.63,-16.47, -15.94 and -15.11. The compound which ranked 2nd according to docking score against wild as well as the three mutants has ZINC database ZINC67912578 and had XP docking score -11.090728, -9.839024, -10.340614 and -11.056422 against 1. 90V94G 2. 74S94G and 3. 90V91P respectively (Table 2). So, taking into the account of large docking score difference and also well-known medicinal properties of CA, all further studies were carried out with it CA only (Table 2).

Entry ID	Wild_XP_docking score	90V94G_XP_docking score	74S94G_xp_docking score	90V91P_xp_docking score	Name
44	-14.64	-16.47	-15.94	-15.11	**Chebulinic Acid** (2-[(4R,5S,7R,8R,11R,12S,13S,21S)-13,17,18-trihydroxy-2,10,14-trioxo-5,21-bis(3,4,5-trihydroxybenzoyloxy)-7-[(3,4,5-trihydroxybenzoyloxy)methyl]-3,6,9,15-tetraoxatetracyclo[10.7.1.1^{4},^{8}.0^{16},^{20}]henicosa-1(19),16(20),17-trien-11-yl]acetic acid)
ZINC67912578	-11.09	-9.84	-10.34	-11.06	{6-[(5,7-dihydroxy-4-methyl-1,2,3,4-tetrahydronaphthalen-2-yl)oxy]-5-hydroxy-3-{[(2E)-3-(4-hydroxyphenyl)prop-2-enoyl]oxy}-4-methyloxan-2-yl}methyl (2E)-3-(4-hydroxyphenyl)prop-2-enoate
ZINC70665965	-10.62	-8.15	-7.66	-7.09	(2S)-1-[(2S)-2-{2-[(2S)-2-[(2R)-2-amino-3-(4-hydroxyphenyl)propanamido]propanamido]acetamido}-3-(1H-imidazol-4-yl)propanoyl]pyrrolidine-2-carboxamide
ZINC04264743	-10.11	-9.01	-11.24	-12.20	[3-({3,5-bis[3,5-bis(hydroxymethyl)phenoxymethyl]phenyl}methoxy)-5-(hydroxymethyl)phenyl]methanol
ZINC68606276	-6.65	-8.36	-7.42	-7.66	2-({4,7,10-tris[(2-hydroxyphenyl)methyl]-1,4,7,10-tetraazacyclododecan-1-yl}methyl)phenol

Table 2: Top five compounds with their docking score against wild and mutant type DNA gyrase enzyme.

5.3 Molecular dynamics simulations studies

A detailed analysis was done to get insights into the binding mode of interaction of CA with each of the four DNA gyrase A enzyme structure. Since molecular docking provides only a static view of the interactions between protein and ligand, molecular dynamics simulations were performed for CA in complex with each protein to study the dynamical behaviour of the interactions. Molecular dynamics simulations gave us the interaction in stable enzyme CA complex, this helped us in deducing the possible mechanism which might cause inhibition of the DNA gyrase enzyme in *Mycobacterium tuberculosis.* The molecular dynamic simulation shows that a Structure of Gyrase A-CA complex for all the wild and three mutant types are stabilized in solvent system and shows a strong binding affinity in the cavity predicted by Q site finder server throughout the simulation duration. Also in all the four complex RMSD was very low and throughout the simulation duration showed low variation. RMSF plot also showed low variation between 50 to 300 residue number, which also comprises our binding cavity (Figure 12, 13, 14 and 15). So, it can be concluded that the complex structures are stable.

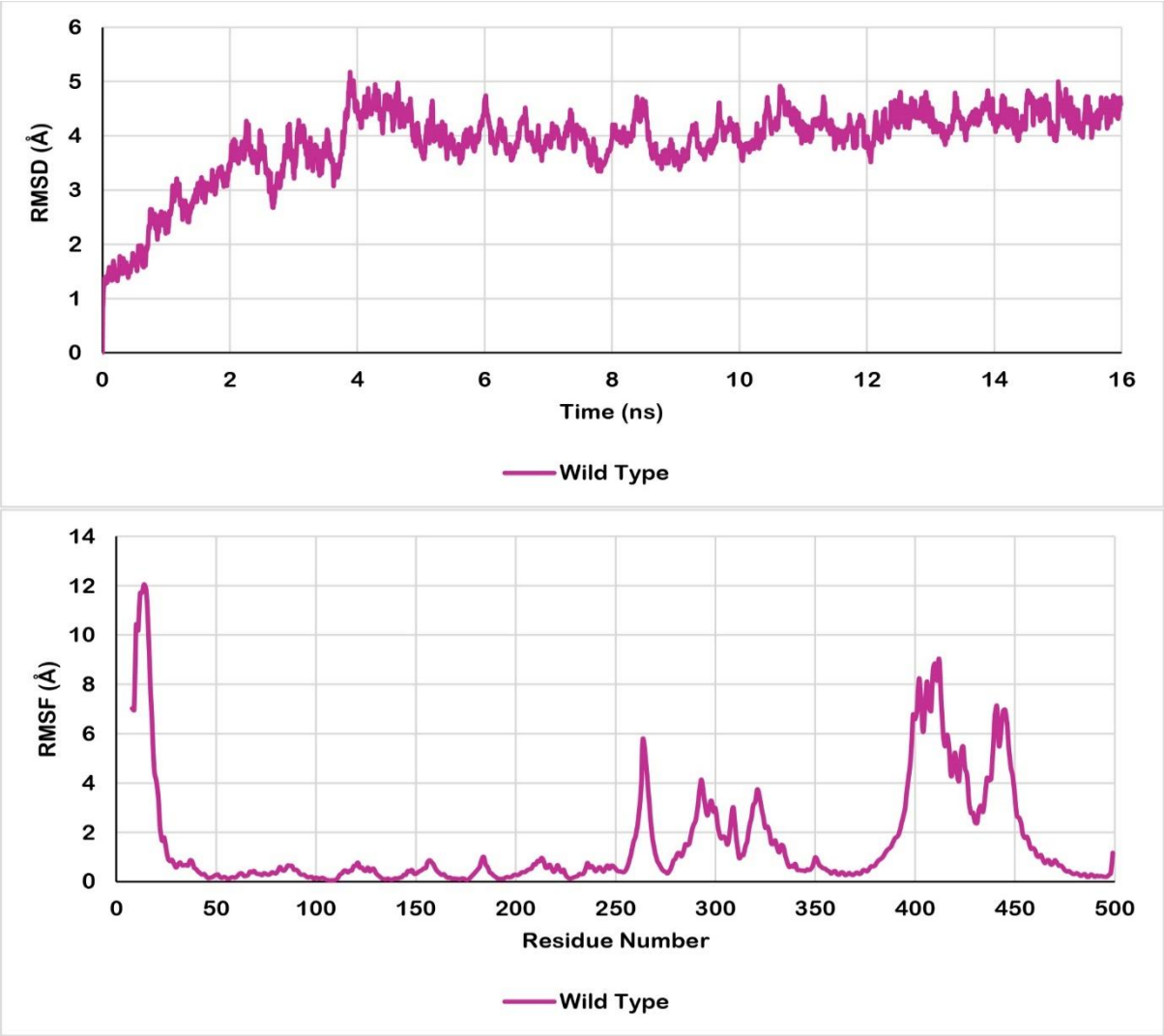

Figure 12: RMSD AND RMSF plot of Wild type DNA gyrA Chain A enzyme after docking and simulation

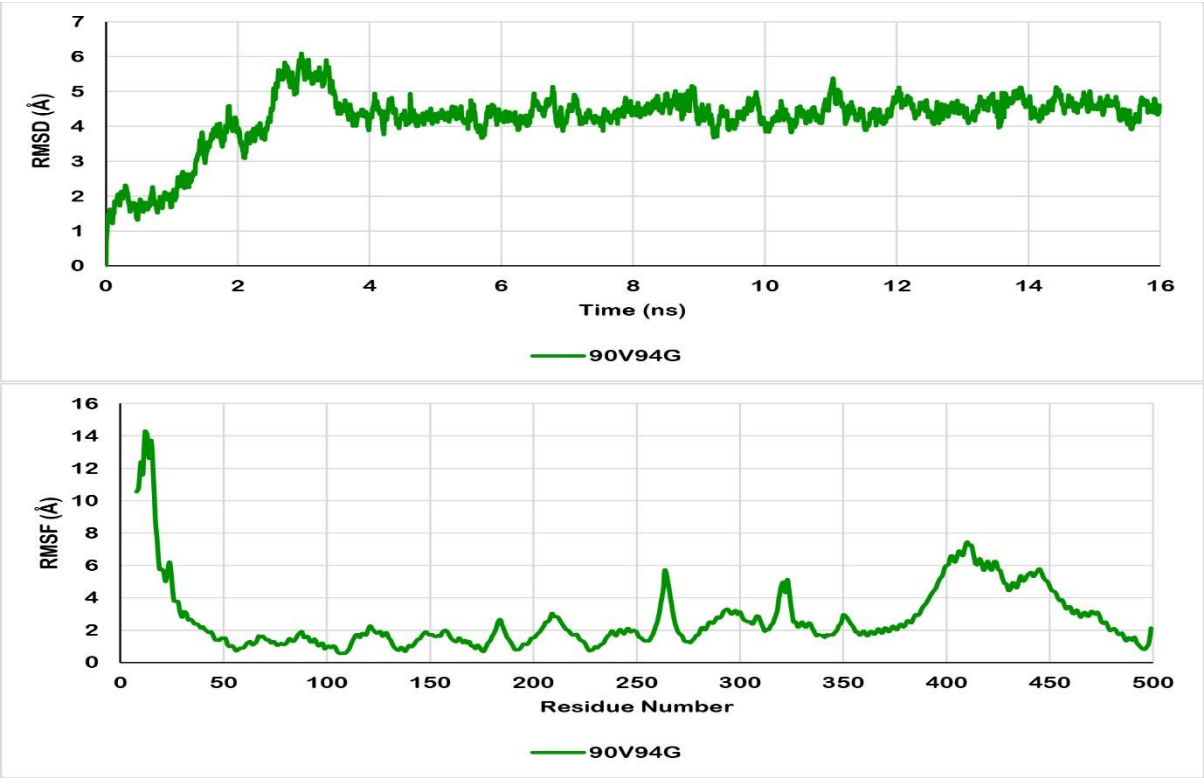

Figure 13: RMSD AND RMSF plot of 90V94G DNA gyrA Chain A enzyme after docking and simulation

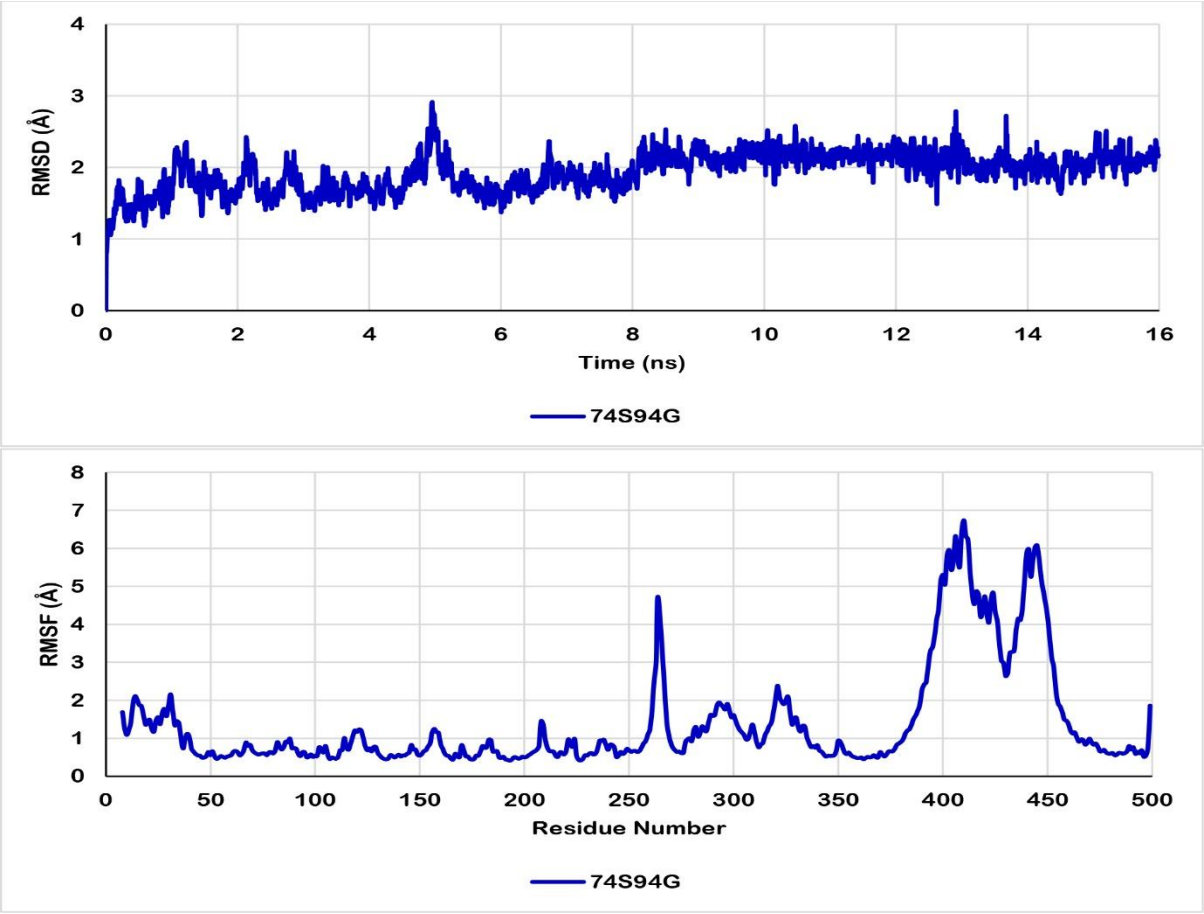

Figure 14: RMSD AND RMSF plot of 7494G DNA gyrA Chain A enzyme after docking and simulation

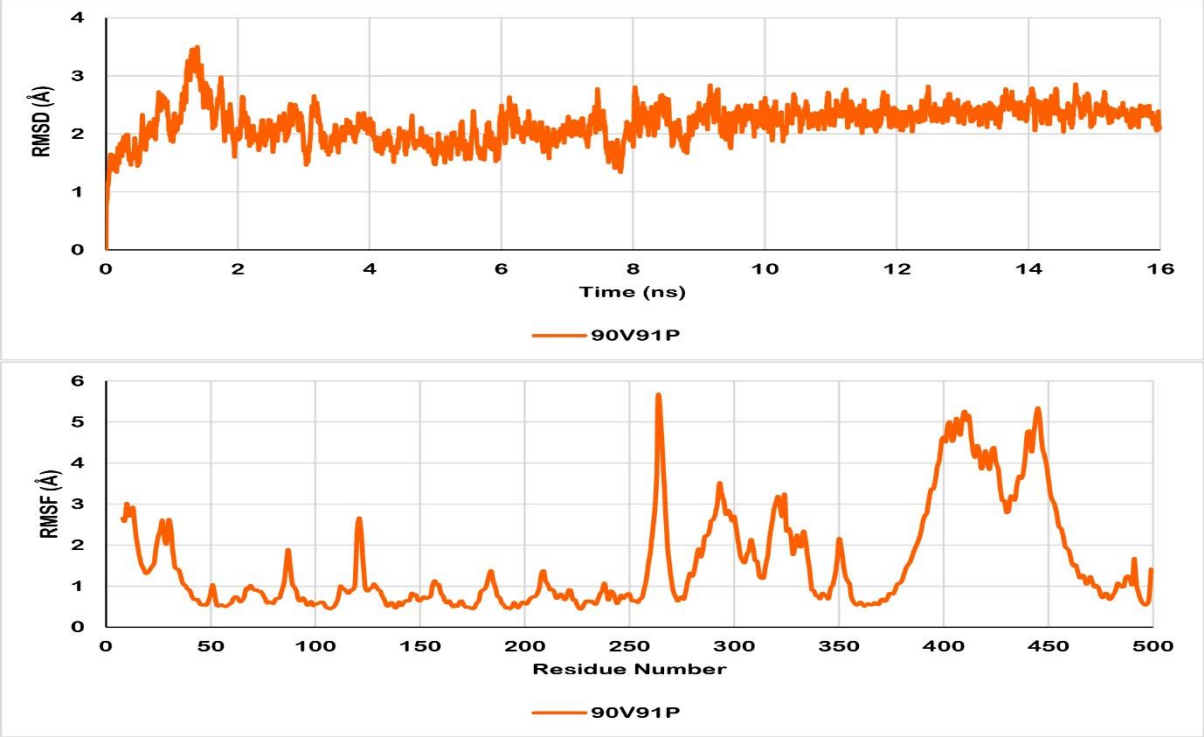

Figure 15: RMSD AND RMSF plot of 90V91P DNA gyrA Chain A enzyme after docking and simulation

CA docked with Wild type Gyrase A has XP docking score of -14.63 and its strong affinity for the selected binding cavity was confirmed by ligplot Protein ligand interaction map which showed 12 H bond between Gyrase A enzyme and CA and hydrophobic interaction with 13 residues (Wallace, Laskowski et al. 1995). During 16ns simulation, dynamic interaction between ligand and enzyme resulted in more stable complex showing 13 H bond between Gyrase A enzyme and CA and 16 residues were involved in hydrophobic interaction. Also, this confirms that even in the presence of solvent the complex is stable (Figure 15 A and B).

In the Molecular Dynamic simulation stabilized structure of 90V94G DNA gyrase A- CA complex, 11 H bonds are formed between the binding cavity of DNA Gyr A and CA and showed a strong interaction. The number of H bond decreased from 12 in docked structure to 11 in representative structure but hydrophobic interaction increased greatly. In docked structure CA was also stabilized by hydrophobic interaction with 8 residues and in representative structure, it increased to 13 residues which made the compound more stable (Figure 16 A and B). Representative structure obtained after allowing the 74S94G DNA gyrase A- CA complex to interact in the presence of solvent for a period of 16ns, 13 H bonds are formed and 17 residues were involved in hydrophobic interaction with the CA. Simulation revealed the dynamic interaction is very strong and is in line with the high -15.9408 XP docking score, 10 H bond formation between ligand and enzyme. The contribution of hydrophobic interaction in stabilization also remained high as 18 residues were involved in interaction before simulation and 17 after the simulation (Figure 17 A and B). Similarly, in the third mutant 90V91P enzyme CA complex, Molecular Dynamic simulation for 16ns revealed the complex is very stable. Even, the number of H-bond halved from 13 before simulation to 6 after simulation, but hydrophobic interaction doubled from 8

to 17 residues involved in the interaction with CA, which indicates a stable enzyme ligand interaction (Figure 18 A and B).

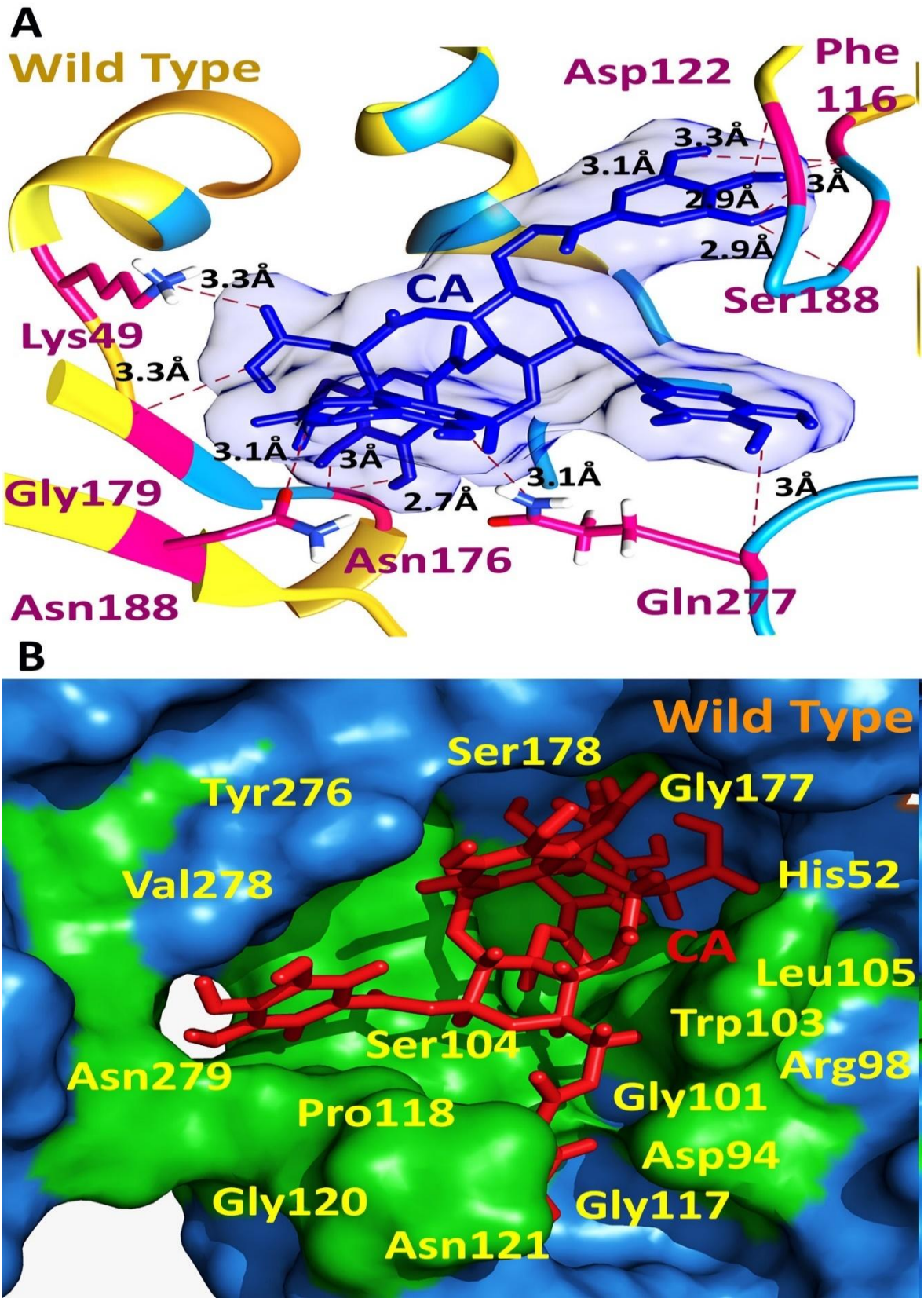

Figure 15: H- bond and hydrophobic interaction. (A) Between CA and binding cavity of Wild type DNA gyrA chain A. (B) Between CA and binding cavity of Wild type DNA gyrA chain A

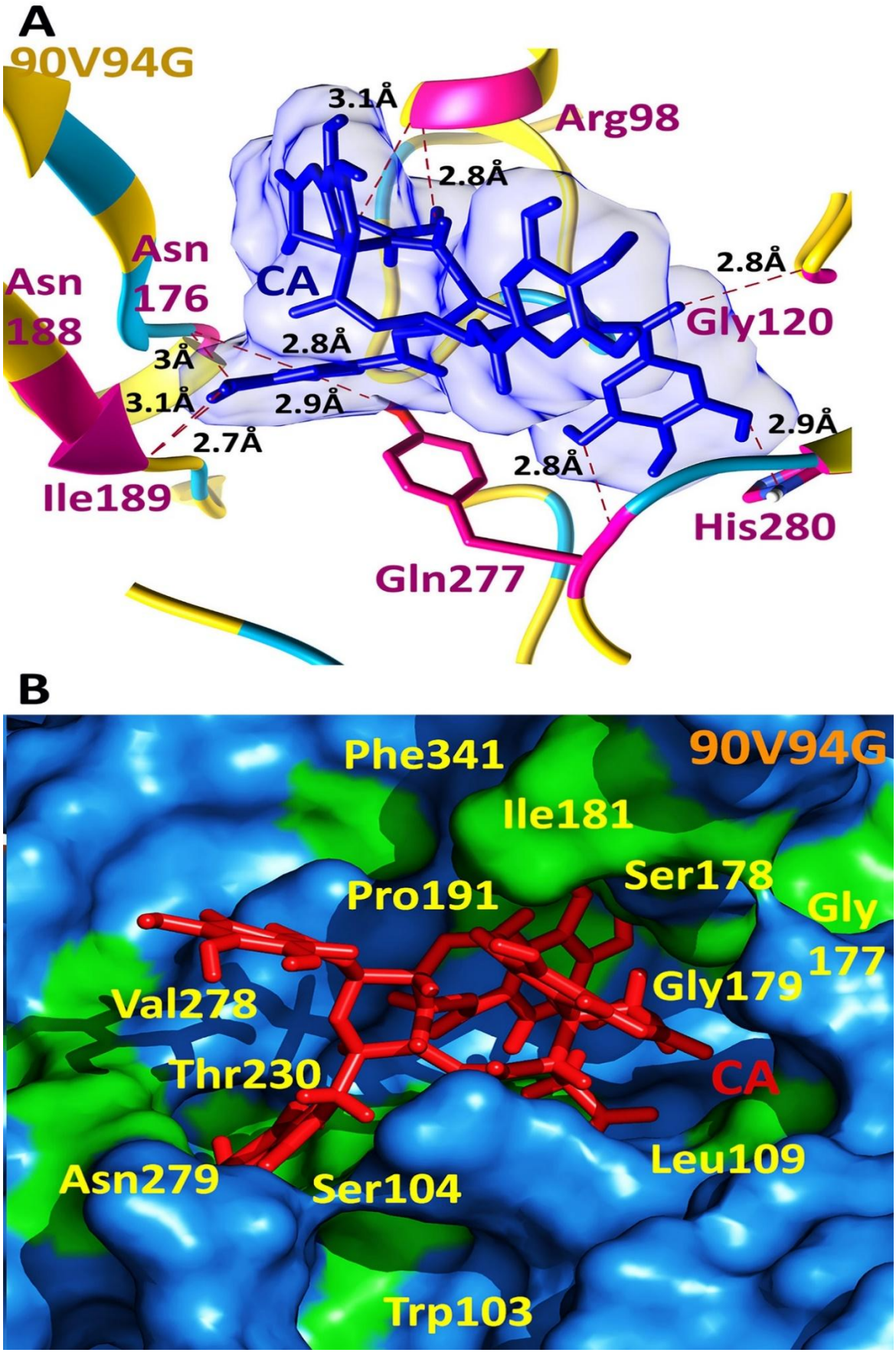

Figure 16: H- bond and Hydrophobic interaction. (A) Between CA and binding cavity of 90V94G DNA gyrA chain A. (B) Between CA and binding cavity of 90V94G DNA gyrA chain A.

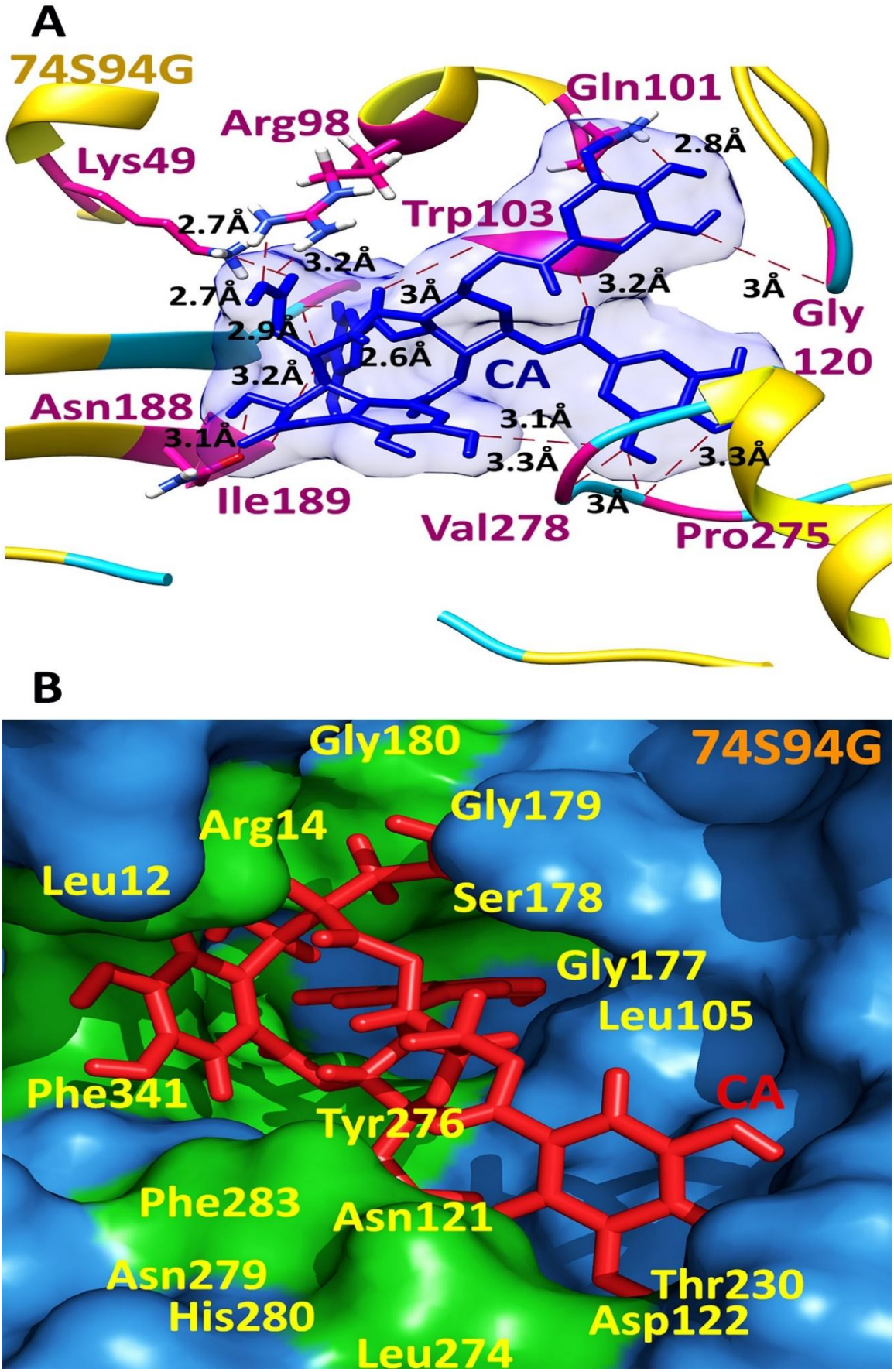

Figure 17: H- bond and Hydrophobic interaction. (A) Between CA and binding cavity of 74S94G DNA gyrA chain A. (B) Between CA and binding cavity of 74S94G DNA gyrA chain A.

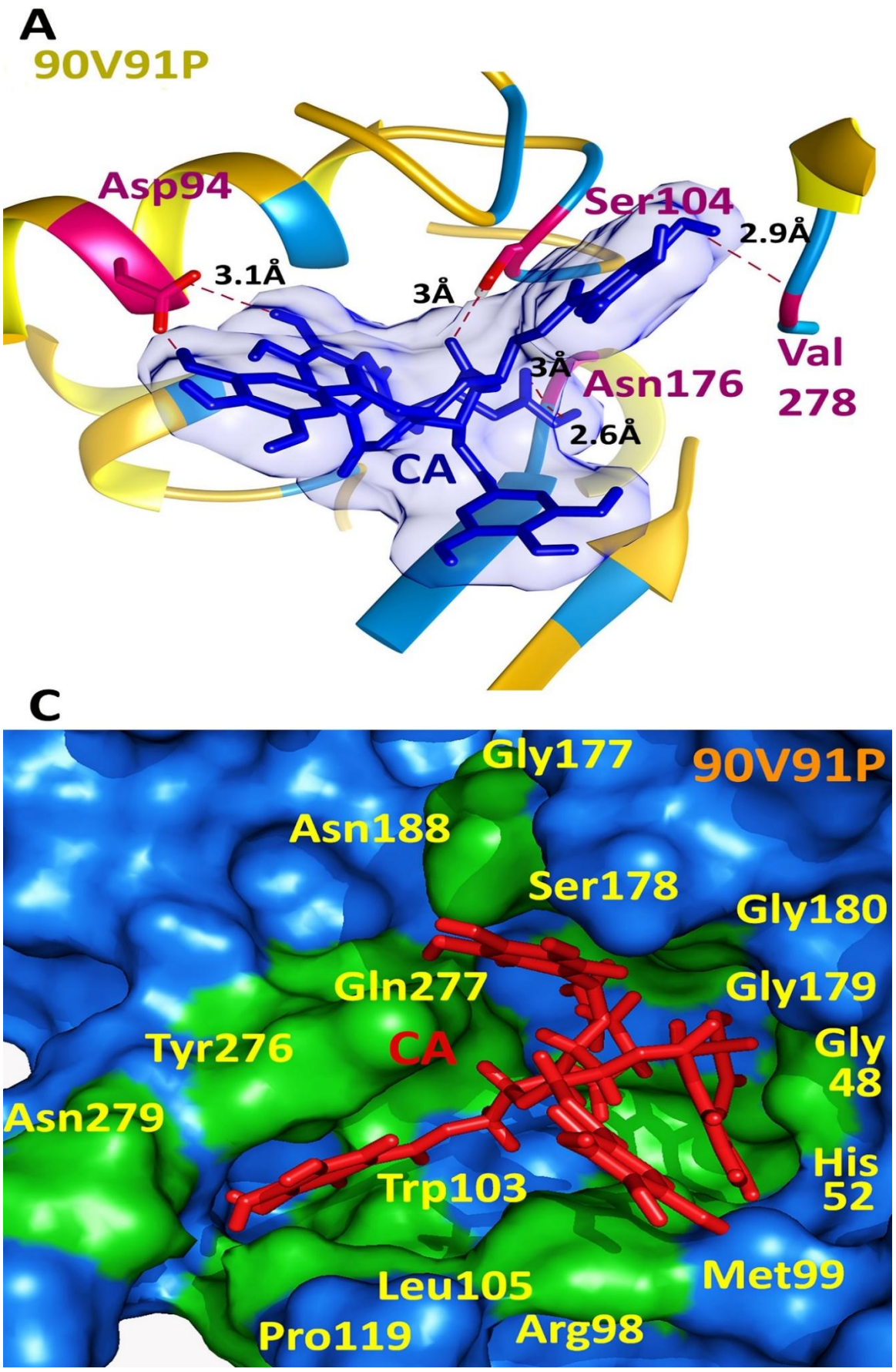

Figure 18: H- bond and Hydrophobic interaction. (A) Between CA and binding cavity of 90V91P DNA gyrA chain A. (B) Between CA and binding cavity of 90V91P DNA gyrA chain A.

All the four complexes showed that the enzyme CA interaction is very stable even in the presence of solvent like water and also has high affinity for the enzyme. The high affinity will make the ligand to bind quickly and will give it an edge in competitive binding against DNA strand which naturally binds at the DNA gate of the DNA Gyrase enzyme.

5.4 Effect of chebulinic acid (CA) on the distance between catalytic residue Tyr129 and phosphate group from DNA

Interruption in H bond formation due to stearic hindrance will lead to improper placement of the DNA in the C gate of DNA gyrase and a less stable complex. Improper binding of DNA will alter the distance between the Tyr129 catalytic residue and the phosphate group from DNA backbone. Tyr129 which performs the cleavage and religation of the DNA strand will be negatively affected by the increase in distance. Inhibition of this cleavage and religation process will make the DNA gyr non-functional. This process will have a fatal effect on the bacterial cell as the DNA replication process will be halted. While comparing with the DNA gyrase-DNA complex modelled protein by tf-modeller, we found that the normal distance between catalytic tyrosine 129 residue and phosphate group of DNA where cleavage occurs is 1.6 Å. However, in the drug-wild type Gyr A complex after Molecular Dynamic Simulation for 16 ns, distance was observed as 5.5Å (Figure 19), in Drug- 90V94G Gyr A, it was observed as 6.1 Å (Figure 22), in drug-74S94G Gyr A complex after MD Simulation for 16 ns, distance was observed as 3.8 Å (Figure 21) and Drug-90V91P Gyr A complex it was observed as 7.3 Å (Figure 22). So we can see in all the four complex there has been a significant increase between the catalytic Tyrosine 129 residue and the phosphate group of the nucleotide. This increase in distance will have an inhibitory effect on catalytic activity of Tyr129 and thus will make the enzyme non-functioning.

5.5 Stearic hindrance at the DNA Gate of DNA gyrase A

The third inhibitory effect of the drug is through stearic hindrance, as shown in figure a major stearic clashes would occur when DNA tries to bind in the DNA gate for cleavage and relegation as the bulk of the CA structure occupies the same space which are required for by the DNA. This will lead to improper placement of DNA strand in DNA gate and will affect the functioning capability of the enzyme (Figure 19, 20, 21 and 22).

Apart from these CA is also involved in hydrophobic interaction with many residues like Leu12, Arg14, His52, Asp94, Arg98, Ala100, Gln101, Ser104, Leu105, Gly117, Pro119, Trp103, Gly120, Asn121, Asp122, Gly177, Ser178, Gly179, Gly180, Thr230, Leu274, Tyr276, Gln277, Val278, Asn279, His280, Phe283 and Phe341 (Figure 15B, 16B, 17B, 18B). Many of these residue are also predicted by the 3dligandsite to interact and stabilise the DNA in the DNA gate by H bond formation, hydrophobic interaction and other weak interaction (Wass, Kelley et al. 2010). Due to the proximity of CA to the DNA binding site and its hydrophobic interaction with the DNA gyrase residue might interfere with the DNA and DNA Gyrase enzyme interaction and have a negative impact the Gyrase enzyme function.

Thus, all the evidences obtained by XP docking and molecular dynamic simulation study suggests that CA has a strong binding affinity for the DNA gyrase enzyme and also can have a strong inhibitory effect on the DNA gyrase and act as a strong anti-tuberculosis drug.

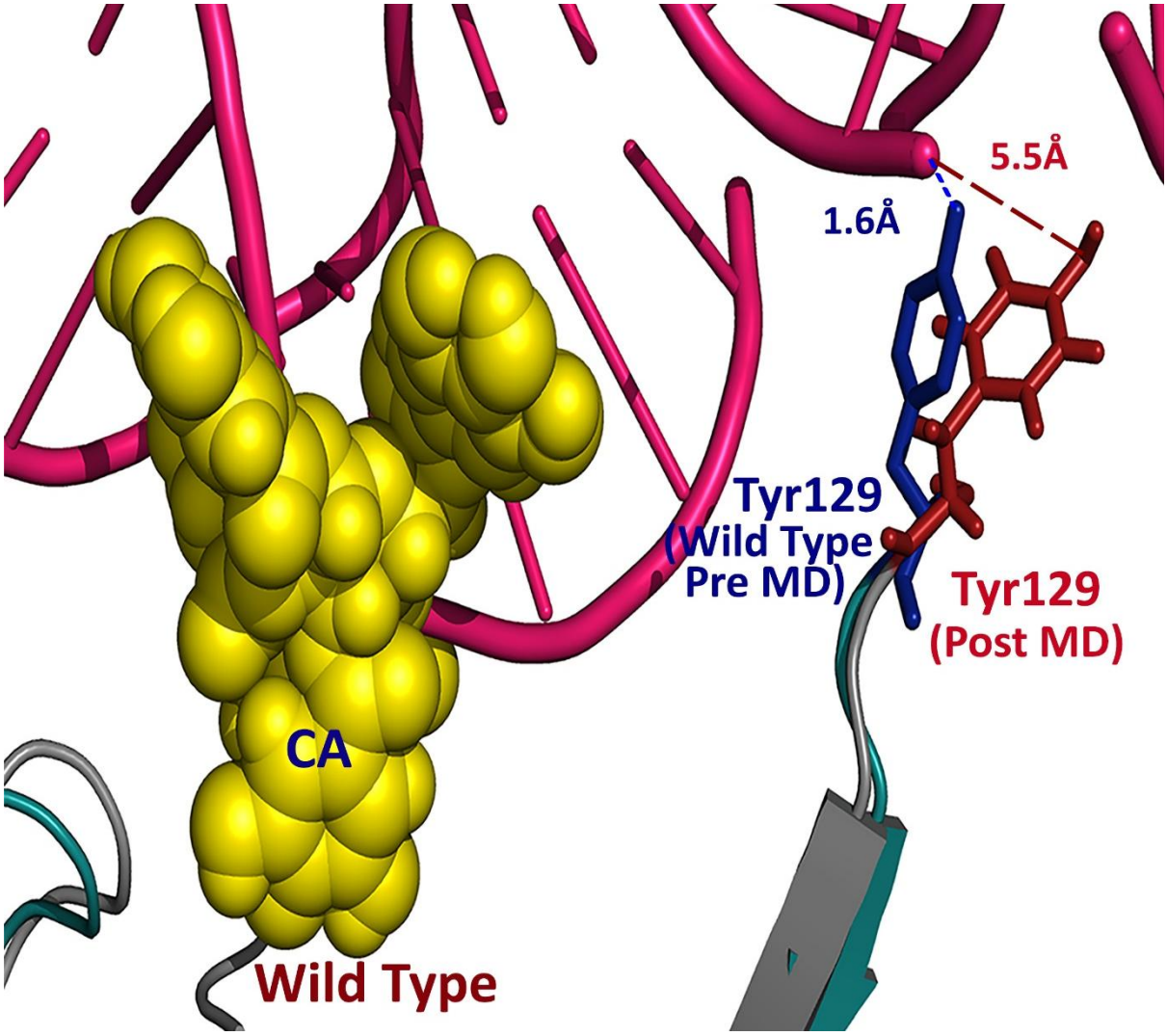

Figure 19: Stearic hindrance between DNA strand at DNA gate and distance between catalytic Tyrosine 129 residue and Phosphate group of DNA in Wild type DNA gyrase A chain A before and after docking and simulation

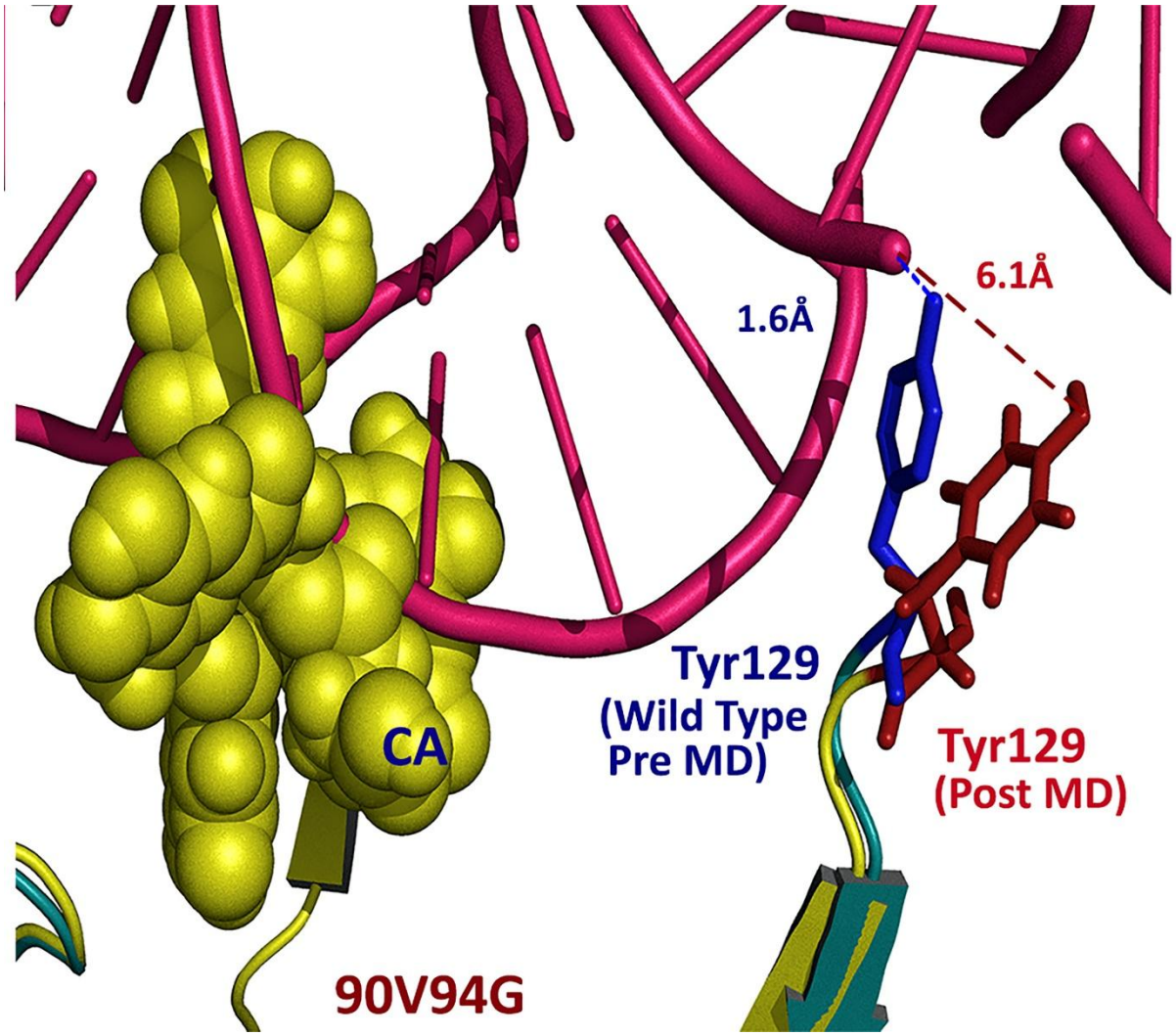

Figure 20: Stearic hindrance between DNA strand at DNA gate and distance between catalytic Tyrosine 129 residue and Phosphate group of DNA in 90V94G DNA gyrase A chain A before and after docking and simulation

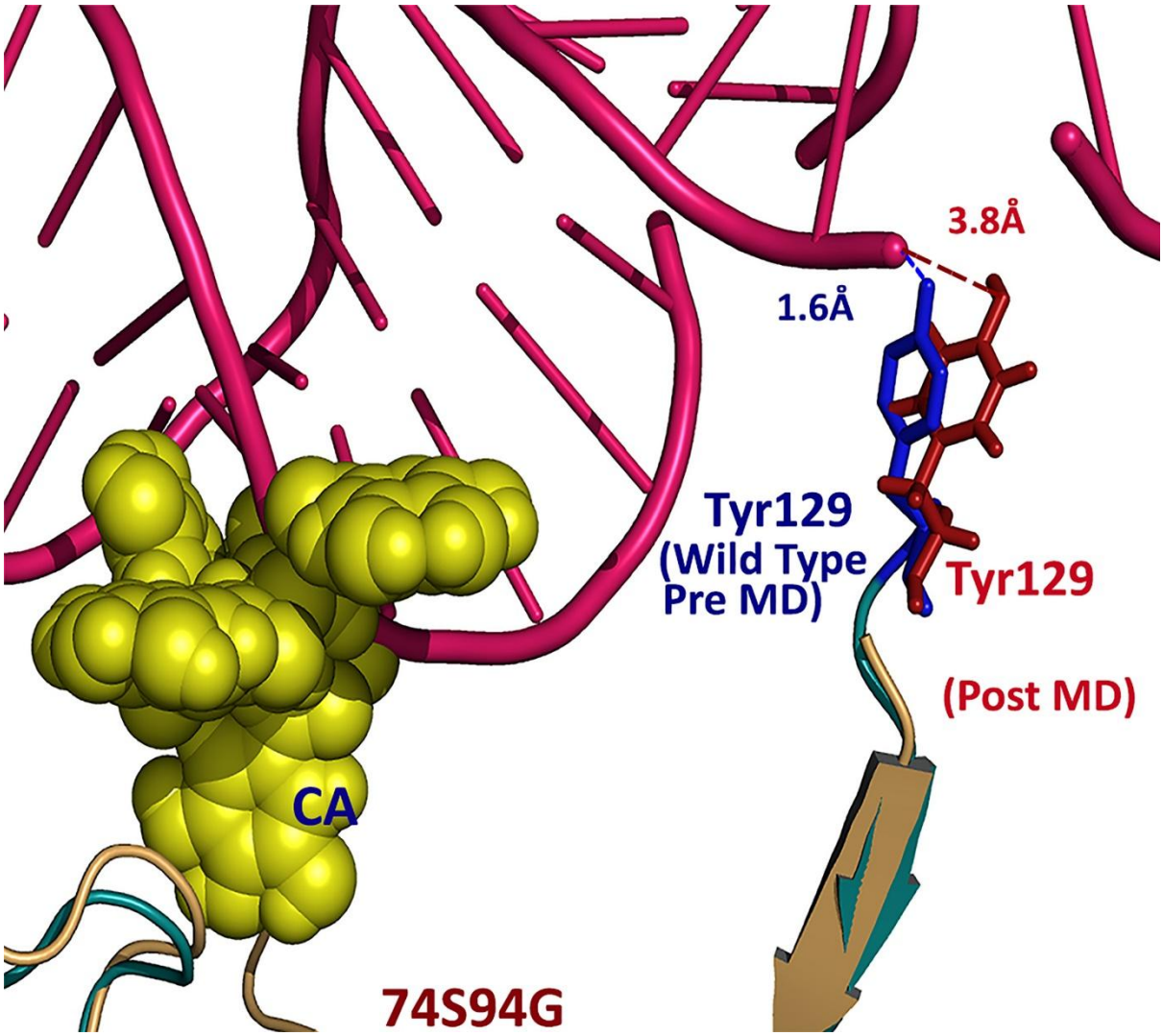

Figure 21: Stearic hindrance between DNA strand at DNA gate and distance between catalytic Tyrosine 129 residue and Phosphate group of DNA in 74S94G DNA gyrase A chain A before and after docking and simulation

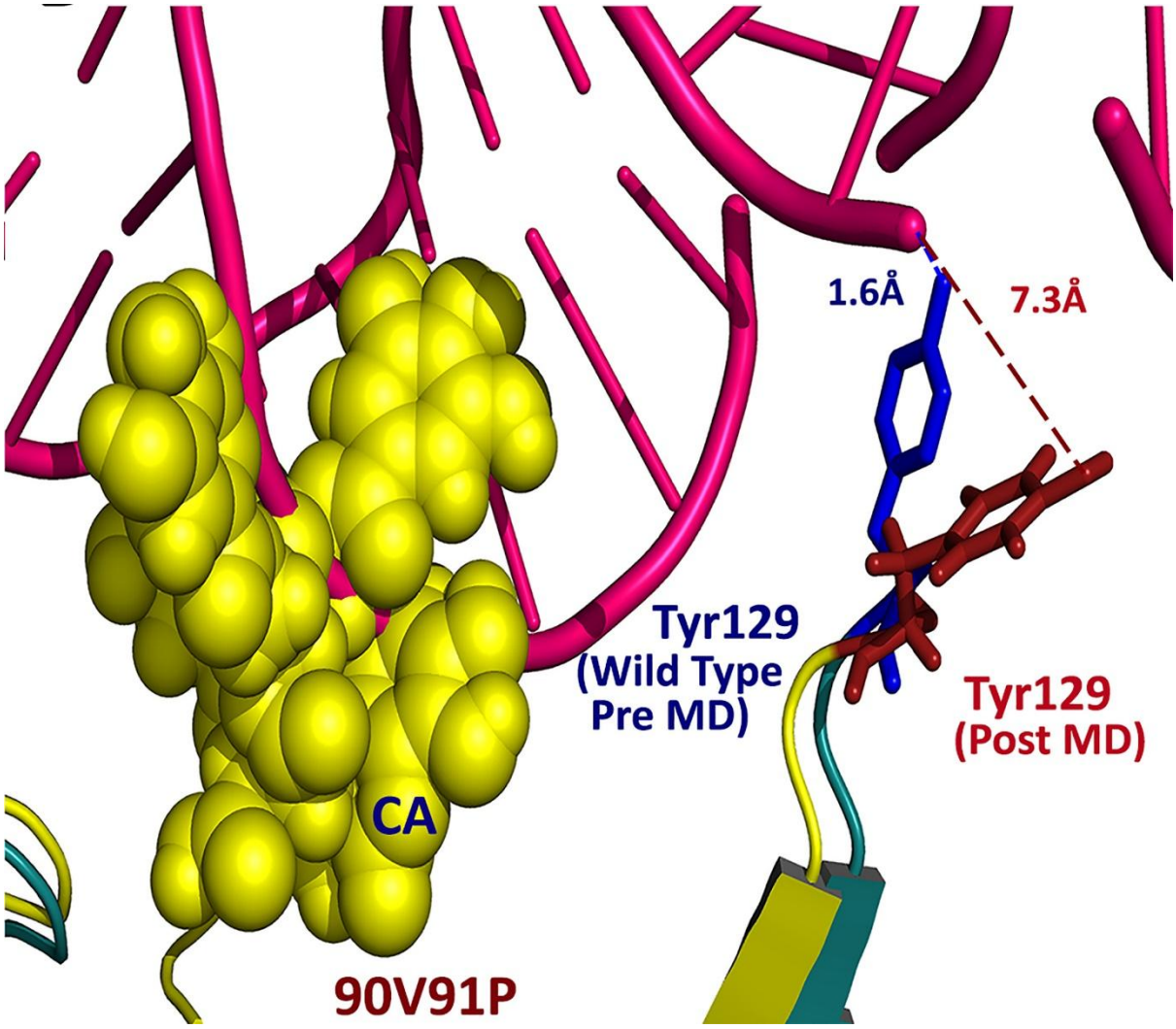

Figure 22: Stearic hindrance between DNA strand at DNA gate and distance between catalytic Tyrosine 129 residue and Phosphate group of DNA in 90V91P DNA gyrase A chain A before and after docking and simulation

6 CONCLUSION AND FUTURE PERSPECTIVE

Tuberculosis and multiple Drug resistant tuberculosis remain as a disease affecting the masses and causing a huge number of deaths every year and is a serious health problem in numerous underdeveloped countries. Due long and complex treatment period cases of MDR TB and XDR TB is on the rise. Identifying suitable drug target is essential for effective drug development. In this study, we have applied the concept of High throughput screening of a phytocompound library against the tuberculosis DNA gyrase which is a unique target and is not present in human and Molecular Dynamic studies to understand the dynamic interaction of drug with the enzyme and its possible effect on the enzyme.

With the absence of double mutant crystal structure, the structure is generated from the wild type DNA gyrase (PDB ID 3IFZ). Energy minimization for all the three double mutations was carried out and further to get a stable structure Molecular Dynamic simulation for 12 ns in the presence of water as a solvent was carried out. A suitable binding site was predicted using Q site server (Laurie and Jackson 2005), ranked one binding cavity was picked as it was most energetically favourable and also present in close proximity to DNA gate. Virtual screening was carried and XP docking using GLIDE protocol was carried out for all wild type and 90V94G, 74S94G and 90V91P double mutant DNA gyrase A. XP results of wild type were compared with all the other three mutant strains in a progressive manner. So that drug candidate obtained in the last was effective against wild as well as other mutants. From 1,79,109 drugs like compound from the Zinc database and Myria-screening database, 2011 compounds were having XP docking score above -6.0 against the wild type and when this was compared with the XP screening results of 90V94G mutant type DNA gyr A, we got 122 compounds which were active against both and had docking score above -6.0 for both. Then this 122 compounds were reduced to 11 when they were compared with 74S94G mutant type DNA gyr A. After the last comparison with the XP docking score of 90V91P, only five drug candidates were obtained which were effective against all the Mutant and wild type DNA gyr A as shown in table 2.

Among them CA was the most effective against all the wild and mutant type DNA gyrase enzymes showing very high XP docking -4.63, -16.46, 15.94 and -15.11 against wild type and 90V94G, 74S94G and 90V91P double mutant DNA gyrase A chain A respectively. Also CA forms a stable complex with all the wild type and mutant type DNA gyr A enzyme by forming 6 to 13 H bonds and multiple hydrophobic interactions. Formation of H bond between CA and DNA gyr A enzyme not only stabilizes the structure, but also negates the possibility of formation of H bond between gyr A enzyme and DNA strand at DNA gate involving these residues. This has a destabilizing effect on the Enzyme DNA complex affecting the catalytic activity of enzyme in a negative way. CA also change the shape of the enzyme in such a way that it increases the distance between catalytic tyrosine residue at the 129 position and DNA from 1.6 Å to 5.2 Å, 6.1 Å, 3.8 Å and 7.2 Å with wild type, 90V94G, 74S94G and 90V91P double mutant DNA gyrase A chain A respectively. Also the bulk of

the CA structure come to the place where DNA strand usually settles at DNA gate. So, along with the increase in distance from catalytic tyrosine residue causing inhibitory effect, stearic hindrance will also cause impairment in the binding of the DNA strand in DNA and cause abnormal binding. This will further not allow the normal functioning of DNA gyrase enzyme and overall cumulatively cause inhibition of the DNA gyrase enzyme. This enzyme inhibition will lead to DNA replication failure in *Mycobacterium tuberculosis* bacteria resulting in its death. This study presents CA as a potential drug candidate for further wet lab validation drug development for treating wild type as well as an MDR and XDR TB.

Chebulinic acid, which has been identified as a common inhibitor. *In vitro* testing of CA on the wild strains and Quinolone resistant mutant strains must be done to find out their IC_{50} of CA. This *in vitro* or *in vivo* testing is necessary to validate the CA as lead compound. Once the inhibitory effect is established, one can go for *in vivo* testing on mice model to study the pharmacodynamics and pharmacokinetics. Also, the dose dependent cytotoxicity effect of CA has to be studied simultaneously. If drug didn't perform well one can go for QSAR study and then for lead optimization to get a better compound having CA properties. Then the final steps of drug designing like clinical trial can be undertaken to complete the process of drug discovery and testing CA's properties as a common inhibitor of TB and MD-RTB.

7 REFERENCES

Al-Sharrah, Y. A. (2003). "The Arab tradition of medical education and its relationship with the European tradition." Prospects **33**(4): 413-425.

Alangaden, G. J., E. K. Manavathu, S. B. Vakulenko, N. M. Zvonok and S. A. Lerner (1995). "Characterization of Fluoroquinolone-resistant mutant strains of Mycobacterium tuberculosis selected in the laboratory and isolated from patients." Antimicrobial agents and chemotherapy **39**(8): 1700-1703.

An, D. D., N. T. H. Duyen, N. T. N. Lan, D. T. M. Ha, V. S. Kiet, N. V. V. Chau, N. H. Dung, D. N. Sy, J. Farrar and M. Caws (2009). "Beijing genotype of Mycobacterium tuberculosis is significantly associated with high-level Fluoroquinolone resistance in Vietnam." Antimicrobial agents and chemotherapy **53**(11): 4835-4839.

Arya, P., R. Joseph and D. T. Chou (2002). "Toward high-throughput synthesis of complex natural product-like compounds in the genomics and proteomics age." Chemistry & biology **9**(2): 145-156.

Aubry, A., L. Mark Fisher, V. Jarlier and E. Cambau (2006). "First functional characterization of a singly expressed bacterial type II topoisomerase: The enzyme from< i> Mycobacterium tuberculosis</i>." Biochemical and biophysical research communications **348**(1): 158-165.

Aubry, A., N. Veziris, E. Cambau, C. Truffot-Pernot, V. Jarlier and L. M. Fisher (2006). "Novel gyrase mutations in quinolone-resistant and -hypersusceptible clinical isolates of Mycobacterium tuberculosis: functional analysis of mutant enzymes." Antimicrob Agents Chemother **50**(1): 104-112.

Baliga, M. S. (2010). "Triphala, Ayurvedic formulation for treating and preventing cancer: a review." The Journal of Alternative and Complementary Medicine **16**(12): 1301-1308.

Bonah, C. (2005). "The 'experimental stable'of the BCG vaccine: safety, efficacy, proof, and standards, 1921–1933." Studies in History and Philosophy of Science Part C: Studies in History and Philosophy of Biological and Biomedical Sciences **36**(4): 696-721.

Burke, M. D., E. M. Berger and S. L. Schreiber (2003). "Generating diverse skeletons of small molecules combinatorially." Science **302**(5645): 613-618.

Capdeville, R., E. Buchdunger, J. Zimmermann and A. Matter (2002). "Glivec (STI571, imatinib), a rationally developed, targeted anticancer drug." Nature Reviews Drug Discovery **1**(7): 493-502.

Carlson, H. A. and J. A. McCammon (2000). "Accommodating protein flexibility in computational drug design." Molecular pharmacology **57**(2): 213-218.

Champoux, J. J. (2001). "DNA topoisomerases: structure, function, and mechanism." Annual review of biochemistry **70**(1): 369-413.

Cheng, A. F., W. W. Yew, E. W. Chan, M. L. Chin, M. M. Hui and R. C. Chan (2004). "Multiplex PCR amplimer conformation analysis for rapid detection of gyrA mutations in Fluoroquinolone-resistant Mycobacterium tuberculosis clinical isolates." Antimicrobial agents and chemotherapy **48**(2): 596-601.

Cole, S., R. Brosch, J. Parkhill, T. Garnier, C. Churcher, D. Harris, S. Gordon, K. Eiglmeier, S. Gas and C. r. Barry (1998). "Deciphering the biology of Mycobacterium tuberculosis from the complete genome sequence." Nature **393**(6685): 537-544.

Control, C. f. D. and Prevention (2006). "Emergence of Mycobacterium tuberculosis with extensive resistance to second-line drugs--worldwide, 2000-2004." MMWR. Morbidity and mortality weekly report **55**(11): 301.

Deep, G., M. Dhiman, A. Rao and R. Kale (2005). "Chemopreventive potential of Triphala (a composite Indian drug) on benzo (a) pyrene induced forestomach tumorigenesis in murine tumor model system." JOURNAL OF EXPERIMENTAL AND CLINICAL CANCER RESEARCH **24**(4): 555.

Donoghue, H. D., A. Marcsik, C. Matheson, K. Vernon, E. Nuorala, J. E. Molto, C. L. Greenblatt and M. Spigelman (2005). "Co–infection of Mycobacterium tuberculosis and Mycobacterium leprae in human archaeological samples: a possible explanation for the historical decline of leprosy." Proceedings of the Royal Society B: Biological Sciences **272**(1561): 389-394.

Espinal, M. A. (2003). "The global situation of MDR-TB." Tuberculosis **83**(1): 44-51.

Essmann, U., L. Perera, M. L. Berkowitz, T. Darden, H. Lee and L. G. Pedersen (1995). "A smooth particle mesh Ewald method." Journal of Chemical Physics **103**(19): 8577-8593.
Farmer, P. (2001). "The major infectious diseases in the world--to treat or not to treat?" The New England journal of medicine **345**(3): 208.
Feher, M. and J. M. Schmidt (2003). "Property distributions: differences between drugs, natural products, and molecules from combinatorial chemistry." J Chem Inf Comput Sci **43**(1): 218-227.
Friesner, R. A., J. L. Banks, R. B. Murphy, T. A. Halgren, J. J. Klicic, D. T. Mainz, M. P. Repasky, E. H. Knoll, M. Shelley, J. K. Perry, D. E. Shaw, P. Francis and P. S. Shenkin (2004). "Glide: a new approach for rapid, accurate docking and scoring. 1. Method and assessment of docking accuracy." J Med Chem **47**(7): 1739-1749.
Garg, A., R. Tewari and G. P. Raghava (2010). "Virtual screening of potential drug-like inhibitors against Lysine/DAP pathway of Mycobacterium tuberculosis." BMC bioinformatics **11**(Suppl 1): S53.
Gutierrez, M. C., S. Brisse, R. Brosch, M. Fabre, B. Omaïs, M. Marmiesse, P. Supply and V. Vincent (2005). "Ancient origin and gene mosaicism of the progenitor of Mycobacterium tuberculosis." PLoS pathogens **1**(1): e5.
Halgren, T. A. (2009). "Identifying and characterizing binding sites and assessing druggability." Journal of chemical information and modeling **49**(2): 377-389.
Halgren, T. A., R. B. Murphy, R. A. Friesner, H. S. Beard, L. L. Frye, W. T. Pollard and J. L. Banks (2004). "Glide: a new approach for rapid, accurate docking and scoring. 2. Enrichment factors in database screening." J Med Chem **47**(7): 1750-1759.
Hegde, S. S., M. W. Vetting, S. L. Roderick, L. A. Mitchenall, A. Maxwell, H. E. Takiff and J. S. Blanchard (2005). "A Fluoroquinolone resistance protein from Mycobacterium tuberculosis that mimics DNA." Science **308**(5727): 1480-1483.
Hershkovitz, I., H. D. Donoghue, D. E. Minnikin, G. S. Besra, O. Y. Lee, A. M. Gernaey, E. Galili, V. Eshed, C. L. Greenblatt and E. Lemma (2008). "Detection and molecular characterization of 9000-year-old Mycobacterium tuberculosis from a Neolithic settlement in the Eastern Mediterranean." PloS one **3**(10): e3426.
Highleyman, L. (1999). "New anti-HIV drugs in development." BETA bulletin of experimental treatments for AIDS: a publication of the San Francisco AIDS foundation **12**(2): 7.
Irwin, J. J. and B. K. Shoichet (2005). "ZINC--a free database of commercially available compounds for virtual screening." J Chem Inf Model **45**(1): 177-182.
Jain, A. N. (2007). "Surflex-Dock 2.1: robust performance from ligand energetic modeling, ring flexibility, and knowledge-based search." Journal of computer-aided molecular design **21**(5): 281-306.
Jorgensen, W. L., D. S. Maxwell and J. Tirado-Rives (1996). "Development and testing of the OPLS all-atom force field on conformational energetics and properties of organic liquids." Journal of the American Chemical Society **118**(45): 11225-11236.
Kaldor, S. W., V. J. Kalish, J. F. Davies, B. V. Shetty, J. E. Fritz, K. Appelt, J. A. Burgess, K. M. Campanale, N. Y. Chirgadze and D. K. Clawson (1997). "Viracept (nelfinavir mesylate, AG1343): a potent, orally bioavailable inhibitor of HIV-1 protease." Journal of medicinal chemistry **40**(24): 3979-3985.
Kaminski, G. A., R. A. Friesner, J. Tirado-Rives and W. L. Jorgensen (2001). "Evaluation and reparametrization of the OPLS-AA force field for proteins via comparison with accurate quantum chemical calculations on peptides." The Journal of Physical Chemistry B **105**(28): 6474-6487.
Laponogov, I., M. K. Sohi, D. A. Veselkov, X.-S. Pan, R. Sawhney, A. W. Thompson, K. E. McAuley, L. M. Fisher and M. R. Sanderson (2009). "Structural insight into the quinolone–DNA cleavage complex of type IIA topoisomerases." Nature structural & molecular biology **16**(6): 667-669.
Laurie, A. T. and R. M. Jackson (2005). "Q-SiteFinder: an energy-based method for the prediction of protein–ligand binding sites." Bioinformatics **21**(9): 1908-1916.
Lee, M. L. and G. Schneider (2001). "Scaffold architecture and pharmacophoric properties of natural products and trade drugs: application in the design of natural product-based combinatorial libraries." J Comb Chem **3**(3): 284-289.

Levine, C., H. Hiasa and K. J. Marians (1998). "DNA gyrase and topoisomerase IV: biochemical activities, physiological roles during chromosome replication, and drug sensitivities." Biochimica et Biophysica Acta (BBA)-Gene Structure and Expression **1400**(1): 29-43.
Lipinski, C. A., F. Lombardo, B. W. Dominy and P. J. Feeney (2012). "Experimental and computational approaches to estimate solubility and permeability in drug discovery and development settings." Advanced drug delivery reviews **64**: 4-17.
Lu, K., D. Chakroborty, C. Sarkar, T. Lu, Z. Xie, Z. Liu and S. Basu (2012). "Triphala and its active constituent chebulinic acid are natural inhibitors of vascular endothelial growth factor-a mediated angiogenesis." PloS one **7**(8): e43934.
Madhavi Sastry, G., M. Adzhigirey, T. Day, R. Annabhimoju and W. Sherman (2013). "Protein and ligand preparation: parameters, protocols, and influence on virtual screening enrichments." Journal of Computer-Aided Molecular Design **27**(3): 221-234.
Malekzadeh, F., H. Ehsanifar, M. Shahamat, M. Levin and R. Colwell (2001). "Antibacterial activity of black myrobalan (< i> Terminalia chebula</i> Retz) against< i> Helicobacter pylori</i>." International Journal of Antimicrobial Agents **18**(1): 85-88.
Migliori, G., R. Loddenkemper, F. Blasi and M. Raviglione (2007). "125 years after Robert Koch's discovery of the tubercle bacillus: the new XDR-TB threat. Is "science" enough to tackle the epidemic?" European Respiratory Journal **29**(3): 423-427.
Montero, C., G. Mateu, R. Rodriguez and H. Takiff (2001). "Intrinsic resistance of Mycobacterium smegmatis to Fluoroquinolones may be influenced by new pentapeptide protein MfpA." Antimicrobial agents and chemotherapy **45**(12): 3387-3392.
O'Hare, T., C. A. Eide and M. W. Deininger (2007). "Bcr-Abl kinase domain mutations, drug resistance, and the road to a cure for chronic myeloid leukemia." Blood **110**(7): 2242-2249.
Oates, J. A., A. J. Wood, D. C. Hooper and J. S. Wolfson (1991). "Fluoroquinolone antimicrobial agents." New England Journal of Medicine **324**(6): 384-394.
Park, H., S. Hong and S. Hong (2012). "Identification of common inhibitors of wild-type and T315I mutant of BCR-ABL through the parallel structure-based virtual screening." Journal of computer-aided molecular design **26**(8): 983-992.
Park, H. and Y. H. Jeon (2007). "Cubic equation governing the outer-region dielectric constant of globular proteins." Physical Review E **75**(2): 021916.
Park, K. (2007). "Park's textbook of preventive and social medicine."
Pawar, V., P. Lahorkar and D. A. Narayana (2009). "Development of a RP-HPLC Method for Analysis of Triphala Curna and its Applicability to Test Variations in Triphala Curna Preparations." Indian journal of pharmaceutical sciences **71**(4).
Piton, J., S. Petrella, M. Delarue, G. André-Leroux, V. Jarlier, A. Aubry and C. Mayer (2010). "Structural insights into the quinolone resistance mechanism of Mycobacterium tuberculosis DNA gyrase." PLoS One **5**(8): e12245.
Raviglione, M. C. and I. M. Smith (2007). "XDR tuberculosis—implications for global public health." New England Journal of Medicine **356**(7): 656-659.
Roberts, N. A., J. A. Martin, D. Kinchington, A. V. Broadhurst, J. C. Craig, I. B. Duncan, S. A. Galpin, B. K. Handa, J. Kay and A. Krohn (1990). "Rational design of peptide-based HIV proteinase inhibitors." Science **248**(4953): 358-361.
Schoeffler, A. J. and J. M. Berger (2008). "DNA topoisomerases: harnessing and constraining energy to govern chromosome topology." Quarterly reviews of biophysics **41**(01): 41-101.
Schrödinger Release 2013-1: Schrödinger Suite 2013 Protein Preparation Wizard; Epik version 2.4, S., LLC, New York, NY, 2013; Impact version 5.9, Schrödinger, LLC, New York, NY, 2013; Prime version 3.2, Schrödinger, LLC, New York, NY, 2013.
SHARMA, R. (2012). Identification of novel inhibitors against Mycobacterium tuberculosis L-aspartate a-decarboxyalse (ADC).
Shi, R., J. Zhang, C. Li, Y. Kazumi and I. Sugawara (2006). "Emergence of ofloxacin resistance in Mycobacterium tuberculosis clinical isolates from China as determined by gyrA mutation analysis using denaturing high-pressure liquid chromatography and DNA sequencing." Journal of clinical microbiology **44**(12): 4566-4568.
Shi, Y., R. P. Sahu and S. K. Srivastava (2008). "Triphala inhibits both in vitro and in vivo xenograft growth of pancreatic tumor cells by inducing apoptosis." BMC cancer **8**(1): 294.

Singh, D., R. Govindarajan and A. Rawat (2008). "High-performance liquid chromatography as a tool for the chemical standardisation of Triphala—an Ayurvedic formulation." Phytochemical analysis **19**(2): 164-168.
Speck-Planche, A., V. V Kleandrova, F. Luan and N. D. Cordeiro (2012). "In silico discovery and virtual screening of multi-target inhibitors for proteins in Mycobacterium tuberculosis." Combinatorial chemistry & high throughput screening **15**(8): 666-673.
Sun, Z., J. Zhang, X. Zhang, S. Wang, Y. Zhang and C. Li (2008). "Comparison of< i> gyrA</i> gene mutations between laboratory-selected ofloxacin-resistant< i> Mycobacterium tuberculosis</i> strains and clinical isolates." International journal of antimicrobial agents **31**(2): 115-121.
van Doorn, H. R., D. D. An, M. D. de Jong, N. T. Lan, D. V. Hoa, H. T. Quy, N. V. Chau, P. M. Duy, D. Q. Tho, N. T. Chinh, J. J. Farrar and M. Caws (2008). "Fluoroquinolone resistance detection in Mycobacterium tuberculosis with locked nucleic acid probe real-time PCR." Int J Tuberc Lung Dis **12**(7): 736-742.
Veziris, N., C. Martin, F. Brossier, F. Bonnaud, F. Denis and A. Aubry (2007). "Treatment failure in a case of extensively drug-resistant tuberculosis associated with selection of a GyrB mutant causing Fluoroquinolone resistance." Eur J Clin Microbiol Infect Dis **26**(6): 423-425.
Viewerlite_5.0 Viewerlite 5.0: Discovery Studio Visualizer**:** Accelrys Inc., San Diago, USA.
Villoutreix, B. O., N. Renault, D. Lagorce, O. Sperandio, M. Montes and M. A. Miteva (2007). "Free resources to assist structure-based virtual ligand screening experiments." Current Protein and Peptide Science **8**(4): 381-411.
Wallace, A. C., R. A. Laskowski and J. M. Thornton (1995). "LIGPLOT: a program to generate schematic diagrams of protein-ligand interactions." Protein engineering **8**(2): 127-134.
Walwaikar, P., V. Morye and A. Gawde (2003). "Ofloxacin in multidrug resistant tuberculosis." Journal of the Indian Medical Association **101**(3): 210-212.
Warren, G. L., C. W. Andrews, A.-M. Capelli, B. Clarke, J. LaLonde, M. H. Lambert, M. Lindvall, N. Nevins, S. F. Semus and S. Senger (2006). "A critical assessment of docking programs and scoring functions." Journal of medicinal chemistry **49**(20): 5912-5931.
Wass, M. N., L. A. Kelley and M. J. Sternberg (2010). "3DLigandSite: predicting ligand-binding sites using similar structures." Nucleic acids research: gkq406.
WHO (2006). The Global Plan to Stop TB 2006-2015: Actions for Life: Towards a World Free of Tuberculosis, Stop TB Partnership.
WHO (2013). Global tuberculosis report 2013, World Health Organization.
WHO (October, 2013). Global Multidrug-resistant tuberculosis (MDR-TB) report 2013, World Health Organization.
Wood, A. J. and M. D. Iseman (1993). "Treatment of multidrug-resistant tuberculosis." New England Journal of Medicine **329**(11): 784-791.
Xu, C., B. N. Kreiswirth, S. Sreevatsan, J. M. Musser and K. Drlica (1996). "Fluoroquinolone resistance associated with specific gyrase mutations in clinical isolates of multidrug-resistant Mycobacterium tuberculosis." Journal of Infectious Diseases **174**(5): 1127-1130.

8 APPENDIX

Table 3: Link to database for top five common inhibitor.

S. No	Compound ID	Web link
1	44 (from self-created library)	http://pubchem.ncbi.nlm.nih.gov/summary/summary.cgi?cid=452240&loc=ec_rcs#x299
2	ZINC67912578	http://zinc.docking.org/substance/67912578
3	ZINC70665965	http://zinc.docking.org/substance/70665965
4	ZINC04264743	http://zinc.docking.org/substance/4264743
5	ZINC68606276	http://zinc.docking.org/substance/68606276

Table 4: RMSF data of wild and mutant strains pre Docking and MD.

Residue number	Wild type (A°)	90V94G (A°)	74S94G (A°)	90V91P (A°)
9	5.716922534	7.962894769	8.974206425	8.218110573
13	8.525339834	9.555282925	10.93335403	11.47685593
17	8.358406433	7.488135073	9.732691864	8.964748153
21	6.998010775	5.880002923	6.453720097	5.826151515
25	4.843108834	4.434366544	3.630284254	4.565303913
29	3.125569801	2.980019457	2.199890117	3.756320488
33	2.310069844	2.476189831	2.025023584	2.760949914
37	2.327583258	1.883713527	1.415687448	2.230160364
41	2.231980882	1.735627104	1.176580965	1.837433268
45	1.71956233	1.412873505	0.970607109	1.496439726
49	1.764669489	1.532831783	1.174402041	1.588523353
53	1.29328499	1.113477234	0.810266597	1.492551315
57	1.274185376	0.939449403	0.778254956	1.739823537
61	1.517894975	1.151337685	1.046694814	1.890183551
65	1.738795913	1.350343656	1.18589675	1.476898116
69	2.0797018	2.047850822	1.637657868	1.542277561
73	1.747513106	1.734981645	0.926709046	1.241540475
77	1.889240061	1.772270357	1.056945091	1.448454377
81	2.509847554	2.224840726	1.381833252	1.803223977
85	2.460419388	1.856282581	1.426802802	1.784350376
89	2.54895131	2.494055582	1.5472744	1.768923076
93	1.814769773	1.711161006	1.077007766	1.209747168
97	1.496254816	1.378697928	1.167450578	1.111190483

101	1.188145212	1.005434483	1.267430604	1.029609932
105	0.94541317	0.842733685	1.161382999	0.932835077
109	0.727955306	0.671360023	0.904558486	0.93500882
113	2.14399011	2.0988351	1.643281015	1.593615434
117	1.735031851	1.622256909	1.502865977	1.143188138
121	3.241247179	2.914171943	2.401331585	2.011636754
125	2.150170104	2.095403722	1.283921708	1.189294869
129	2.74848637	2.717786986	1.67744978	1.812877116
133	1.45944496	1.229148925	1.104295898	1.219973823
137	1.159773425	1.193070989	1.231452504	1.227479403
141	0.770182875	0.836119192	0.910007043	1.175572628
145	1.276642134	1.073921335	0.869845169	1.86136288
149	1.560368011	1.280885895	0.793966816	1.66193811
153	2.131538923	1.60332558	1.172417166	2.444012077
157	2.708273201	2.107479341	1.761013442	3.055131303
161	1.948183232	1.504410399	1.201040802	2.578022799
165	1.427017965	1.179947711	0.766797727	1.523681574
169	1.219582894	1.128295781	0.961653293	1.290315665
173	1.317213229	1.272719312	1.051582236	0.993599774
177	1.018765701	0.984879584	1.076514829	0.900451951
181	2.111788877	1.8878383	1.804099336	1.992994901
185	2.271789565	2.136510977	1.681170865	2.340736481
189	1.327487219	1.199701646	1.155874039	1.157232074
193	1.079857734	1.010014757	1.160899655	0.827402962
197	1.371209169	1.164968696	1.319424907	0.702966678
201	1.505225115	1.407738588	1.049651563	0.729660031
205	1.859264868	1.639610298	1.052627572	0.961110493
209	2.803424218	2.474126448	1.976646582	1.971034045
213	2.891483888	2.856578277	2.332047306	1.999757754
217	2.311575856	2.099914381	1.604558771	1.377317418
221	1.968521839	1.742456055	1.732961178	1.510209401
225	1.295987439	1.253687268	1.369148126	1.038413548
229	1.017315862	0.901056689	1.275855015	0.924267185
233	1.616882848	1.45243828	1.728557022	1.731117195
237	2.298241183	2.019150329	2.041665089	2.106505428
241	2.132983794	1.888029627	1.86778628	1.818061369
245	2.377932162	2.210625042	1.895884234	1.834193913
249	1.956504226	1.744349645	1.607529802	1.716945897
253	1.727781019	1.399103193	1.948240915	1.837999248
257	2.112859296	1.878958442	2.156108498	2.183404197
261	4.031048947	3.205536853	3.784621336	4.096647078

268	2.87961083	2.273918347	2.83721867	2.490294241
272	2.143438924	2.124948286	2.541021571	1.602697298
276	1.39538696	1.374852293	1.547056331	1.216839043
280	2.421960041	1.899867707	2.675783675	1.486970292
284	2.605117243	2.089459602	3.098028024	2.187582832
288	3.035220301	2.72826765	3.401387957	2.270532921
292	3.904294106	4.115467978	4.242795299	3.310644225
296	3.14387423	3.041663943	2.727501355	2.984478571
300	3.724670154	2.79414154	3.551573187	2.878705257
304	2.966607493	2.543298131	4.305212297	1.957283722
308	3.944886413	4.566790511	5.183152164	3.589982177
312	2.297913731	2.451213039	3.150494379	2.051850476
316	2.688886332	2.070759515	2.665580951	2.22012061
320	4.375098417	3.245819733	4.395607423	4.382506297
324	3.051968835	3.50269013	2.442331591	4.127240468
328	2.452638606	2.120432568	2.004980284	3.082467007
332	2.237283722	1.898981288	2.100731163	2.648801033
336	2.366787914	2.028781296	2.848988467	3.282908913
340	1.908300636	1.597571435	1.914912346	1.926611191
344	1.920354095	1.745083309	1.466117578	1.733044579
348	2.357313259	1.562510903	1.148846601	2.515564741
352	2.880922315	2.035561752	1.550539482	2.987305077
356	1.92358221	1.87179677	1.316661666	1.522067941
360	1.939004091	1.814892498	1.21932679	1.234775308
364	2.270914459	1.817024136	1.368909772	1.52652451
368	1.590525274	1.322361826	0.899419276	1.221824993
372	1.578602495	1.357334786	0.764925309	1.395850025
376	1.783368054	1.522613129	1.01108558	1.708518713
380	2.205640567	1.767651619	1.226707285	2.078643107
384	3.016195761	2.206309116	1.741322273	2.660965746
388	3.681138591	2.690656169	2.276557599	3.201770953
392	4.621070837	3.24546885	2.593012571	3.720243168
396	6.437152798	4.782229643	3.663306703	4.723812263
400	8.037111336	6.105112549	4.682640108	5.507601491
404	7.738003637	5.875771927	4.699334674	5.472907373
408	7.797219212	6.229067307	4.941756937	5.603024902
412	8.583315007	7.195054425	6.455699537	6.564618566
416	7.290623394	5.804487383	5.344154423	5.8759878
420	7.10224761	5.262262153	4.772934015	5.546570798
424	7.666945198	5.596447823	4.771634454	5.693179421
428	4.96537219	3.758051669	3.478432147	4.326933775

Table 5: RMSF data of wild and mutant strains post Docking and MD.

Residue number	Wild type (A°)	90V94G (A°)	74S94G (A°)	90V91P (A°)
9	6.963742709	10.83955137	1.262777198	2.583748906
13	11.71794103	14.10357782	1.907878126	2.910438162
17	8.17412617	8.935741945	1.845441515	1.528677387
21	3.520276087	5.612156405	1.483606043	1.401187854
25	1.349624917	5.07069968	1.551112461	2.207714549
29	0.718965033	3.129688218	1.578050943	2.03057989
33	0.672400091	2.631777704	1.339128218	1.464682493
37	0.870713647	2.391326554	0.729478627	1.046904826
41	0.416920999	2.038743995	0.725957794	0.766837304
45	0.224752466	1.672475415	0.540261933	0.565897014
49	0.240524122	1.519920431	0.636159058	0.639895661
53	0.16164823	0.987427308	0.457904519	0.535252988
57	0.151289766	0.783211723	0.487511834	0.503939831
61	0.264135049	1.128947346	0.645277049	0.706850721
65	0.241718682	1.166030562	0.587210783	0.649095407
69	0.441902745	1.626258098	0.826067067	1.017690122
73	0.269049037	1.209182556	0.569986128	0.875562753
77	0.305714234	1.121239947	0.554832751	0.592557192
81	0.449148481	1.297886373	0.679435226	0.684996436
85	0.539267209	1.478606216	0.761659185	1.065304602
89	0.489945302	1.547435688	0.738126063	1.057213963
93	0.284185143	1.271445802	0.530731299	0.646876335
97	0.196340406	1.152112487	0.511318841	0.559385875
101	0.147845998	1.009765973	0.53233387	0.573489453
105	0.086036387	0.696755221	0.797569212	0.492618572
109	0.067127564	0.578215271	0.477496889	0.506637957
113	0.339567265	1.465496792	0.691136329	0.947138732
117	0.448754798	1.7795849	0.858493695	0.906660888
121	0.777653083	2.262311848	1.229665298	2.661521296
125	0.4462052	1.858582343	0.684669192	0.880959339
129	0.528143881	1.83523161	0.77019215	0.993093522
133	0.143199044	0.899212451	0.455916021	0.668134837
137	0.098270552	0.816213058	0.536470373	0.579003503
141	0.138460877	0.973131718	0.520592702	0.528799629
145	0.28609741	1.463233044	0.62497381	0.6495852
149	0.343284138	1.762739333	0.570593224	0.661350133
153	0.473326827	1.611920547	0.685774743	0.700177036
157	0.871003645	1.977415242	1.245479798	1.133062555

161	0.413482451	1.399701016	0.724475786	0.761874605
165	0.225361371	1.384105651	0.459086441	0.543058039
169	0.139982691	1.291487387	0.501892449	0.623747628
173	0.137348872	1.072813715	0.523055116	0.493100506
177	0.145481719	0.932428195	0.543083152	0.58493609
181	0.497572012	1.806744169	0.747412743	0.935797022
185	0.703198111	2.284084108	0.650100773	1.113842786
189	0.25192334	1.262369703	0.481744492	0.589532784
193	0.12427743	0.8024304	0.407558914	0.455203484
197	0.17805412	1.119036846	0.463918585	0.478939233
201	0.266442819	1.61256031	0.508855358	0.57056403
205	0.410599376	2.249736398	0.657022644	0.752740217
209	0.705502777	3.041168317	1.367533745	1.377096912
213	0.967995337	2.571333921	0.654858112	0.923031346
217	0.696332662	1.974020095	0.625650017	0.804975288

Table 6: RMSD data of wild and mutant strains pre Docking and MD for 12ns.

time (ns)	Wild type (A°)	90V94G (A°)	74S94G (A°)	90V91P (A°)
0	2.40082E-14	1.31833E-14	2.77801E-14	7.43145E-15
0.160032	1.731663716	1.952858652	1.788645854	1.533521224
0.320064	2.154742469	1.933363767	1.87621525	1.879793951
0.480096	3.098951507	2.808965113	2.269257135	2.037150135
0.640128	3.384271124	2.877952735	2.196877767	2.655684457
0.80016	3.109653756	3.153373244	2.396204058	2.831005298
0.960192	2.912913723	2.698139287	2.980890238	2.592393128
1.120224	2.928846196	2.706652381	3.220922044	3.281515518
1.280256	2.618374746	2.60050072	3.253989256	3.110554941
1.440288	2.979179821	2.683594358	3.522612902	4.052429394
1.60032	3.167247904	3.126585623	3.72150107	3.243761129
1.760352	3.823662596	2.949107326	3.563787518	3.669926421
1.920384	3.043582435	3.081338551	3.803300268	3.698974271
2.080416	3.480812344	3.047810867	3.700266698	3.636960683
2.240448	3.130681435	3.507157081	3.855478457	3.89392691
2.40048	3.464746224	2.859501735	3.759834764	3.878615406
2.560512	3.968788257	2.950399497	4.257764019	4.348660988
2.720544	3.972051683	3.251469741	4.377527144	4.573159024
2.880576	4.105821118	3.742726551	4.286551239	4.540985717
3.040608	3.850704339	3.810825488	4.620929314	4.620840585
3.20064	3.409814969	3.934951294	4.6113546	4.772195824
3.360672	3.574908131	4.40933271	4.401181266	4.464599029
3.520704	4.209714494	4.411944391	4.445528548	4.344267075
3.680736	4.25056156	4.627304066	4.142596152	5.298121142
3.840768	3.808299589	4.457840067	4.263361379	5.201884473
4.0008	3.840767275	4.809937284	4.494449647	5.074257983
4.160832	4.076653074	4.548342398	4.684663246	4.733088168
4.320864	3.896079971	5.034795792	4.107574401	5.043946596
4.480896	3.897097348	5.23506201	4.518827765	5.313331287
4.640928	4.090233058	5.176619951	4.844005972	5.024203867
4.80096	4.518054827	5.255383696	4.987782482	5.033451026
4.960992	4.352587574	4.632187147	5.09899836	5.026076255
5.121024	3.85787897	5.153114489	4.868540356	4.958974956
5.281056	3.797463407	5.442181269	4.859740428	4.916674774
5.441088	3.310825464	4.857963547	4.840136264	4.835317966
5.60112	3.502135338	4.615420661	5.05049961	4.598873046
5.761152	3.425544693	4.244367866	5.446640431	4.223649425
5.921184	3.744597547	4.759214912	5.079427345	4.453366496
6.081216	3.178103627	4.803636415	5.145449174	4.457204552
6.241248	3.936394615	4.629158096	5.364231799	4.575666744
6.40128	3.828748319	4.723422343	5.565777034	4.51148569

6.561312	3.397503427	4.724242627	5.804512678	4.167816441
6.721344	3.931514997	4.101538477	5.562893934	3.571010423
6.881376	4.420242965	3.898870639	5.637275277	3.911031184
7.041408	4.373396625	4.335732098	5.959887422	4.226176992
7.20144	4.296419697	4.408292236	5.950819308	4.168683057
7.361472	4.170356382	4.539178461	5.811535465	3.943849904
7.521504	3.971482155	4.598121664	6.048741517	4.286216388
7.681536	3.967729009	4.281300206	5.806071573	4.524248605
7.841568	4.213297507	4.698150178	6.243653287	4.763154232
8.0016	3.869097213	4.889350423	5.926546455	4.905181435
8.161632	4.268964055	4.988945478	5.692945308	4.606948219
8.321664	3.876459414	4.692448471	5.618084817	4.970750853
8.481696	3.842413023	4.403912105	5.791334512	5.193588844
8.641728	4.431762727	4.141152892	6.062277881	4.733499844
8.80176	4.134980278	4.318641203	5.904959926	4.834718393
8.961792	4.065352527	4.454546947	6.084234776	5.435625925
9.121824	4.188687862	4.523839642	6.272977586	5.372559077
9.281856	4.350191776	4.46058036	5.971860163	5.727873839
9.441888	4.036861097	4.441436854	6.086579758	5.523067898
9.60192	4.372504252	4.544817668	6.139094028	5.662360095
9.761952	4.536414525	5.459794162	6.223920832	5.640822905
9.921984	3.957734444	5.387820568	6.366647613	5.893026803
10.090018	4.299435711	5.435375284	6.473567537	6.248670549
10.25005	4.06045543	4.781937062	6.263812244	6.017871345
10.410082	4.486212969	5.348093974	6.452441191	6.218556853
10.570114	4.50387845	5.407633877	6.702047126	6.41157597
10.730146	4.589623391	5.038573883	6.373642907	6.227701135
10.890178	4.389212524	5.02712807	6.203410729	6.179894747
11.05021	4.374274745	4.914645632	6.269215027	6.416117039
11.210242	4.262910223	4.982399052	6.79982893	6.01387589
11.370274	4.140638919	5.08307418	6.255057352	5.820131845
11.530306	4.056996866	4.702177429	6.095450427	5.550304823
11.690338	4.467234212	5.113214895	6.60133136	5.808647214
11.85037	4.471406974	5.064937013	6.576779777	5.99637903

Table 7: RMSD data of wild and mutant strains post Docking and MD for 16ns.

time (ns)	Wild type (A°)	90V94G (A°)	74S94G (A°)	90V91P (A°)
0	8.79E-15	7.98E-15	5.90E-15	6.78E-15
0.0768	1.311146142	1.467690249	1.0907602	1.536966018
0.1536	1.430241469	1.81048291	1.403695661	1.351892717
0.2304	1.354283486	2.131198391	1.597035965	1.810790927
0.3072	1.59414619	2.279923295	1.244607827	1.844971179
0.384	1.475461919	1.689305394	1.482813717	1.591949541
0.4608	1.685603025	1.470415652	1.540434074	1.751669983
0.5376	1.687092852	1.746241487	1.802692559	1.909629335
0.6144	1.957801427	1.724941998	1.452778491	1.869059285
0.6912	1.957196605	2.045248577	1.585573482	2.143046294
0.768	2.623677439	1.624584864	1.556821475	2.248081915
0.8448	2.404648013	1.725613417	1.586696318	2.62285975
0.9216	2.601843787	2.015641787	1.758239906	2.501290411
0.9984	2.286773487	1.682129907	1.722055493	1.996829692
1.0752	2.58880469	2.204093855	2.206849392	2.12762742
1.152	3.017593519	2.629065956	1.735674232	2.487361916
1.2288	2.715843072	2.440946096	2.166044933	3.119286378
1.3056	2.623823085	2.556539861	2.015263109	3.454827791
1.3824	2.590066683	3.033039138	1.712632708	3.346249713
1.4592	2.905524363	3.836241427	1.35113877	2.956519523
1.536	3.151976688	3.283495467	1.870473887	2.826744292
1.6128	2.812420947	3.627746793	1.808227294	2.255884153
1.6896	3.042383054	4.062577214	1.959675979	2.518571981
1.7664	2.918506593	3.408972695	1.511983414	2.684673011
1.8432	3.297069833	4.018664934	1.441508478	2.094702674
1.92	3.166106885	3.911976449	1.585099856	2.034909864
1.9968	3.368931786	3.87339641	1.642499206	2.088906658
2.0736	3.696251322	3.301772203	1.699242706	2.584968119
2.1504	3.775183371	3.679311809	2.263084352	2.283282599
2.2272	3.683792168	3.799210927	2.191006352	2.016508525
2.304	3.736090685	3.781723453	1.58244468	1.997873953
2.3808	3.641308029	3.721071392	1.695854052	2.242908511
2.4576	3.561707063	4.148417591	1.843407257	2.07600338
2.5344	3.647088827	4.565563209	1.544367161	1.683342397
2.6112	3.250911532	5.406202313	1.549988933	2.032102518
2.688	2.826343709	5.413207544	1.607955773	2.226449631
2.7648	3.101422129	5.65040325	1.947534532	2.055376682
2.8416	3.39182914	5.145010229	1.901172453	2.311231893
2.9184	4.096393602	5.637985307	1.779400057	2.096651295
2.9952	3.319028872	5.795164645	1.573724732	1.932136852
3.072	4.109722989	5.918669282	1.601057654	1.699058481

3.1488	4.125003067	5.253980118	1.473498461	2.320335179
3.2256	3.518053094	5.428224276	1.58537306	2.328720092
3.3024	3.351726715	5.322694536	2.021675105	2.025182019
3.3792	3.633346766	5.648407485	1.896278459	1.634843267
3.456	3.622261443	4.95081842	1.858155093	1.973455877
3.5328	4.080582482	4.625590517	1.528272491	1.811595992
3.6096	3.577029602	4.62137427	1.829279068	1.980639827
3.6864	3.289013186	4.178492671	1.763946073	2.038919735
3.7632	3.655382882	4.055460233	1.635615354	2.123013077
3.84	4.336426124	4.354630312	1.651713859	2.290417744
3.9168	4.83640468	4.310212567	1.812299163	2.291766935
3.9936	4.457494569	4.040124238	1.627168033	2.066829081
4.0704	4.171920348	4.61981941	1.569088031	1.891566919
4.1472	4.358284342	4.414123731	1.654638595	1.76378901
4.224	4.395191828	3.958193399	1.687155968	1.886193423
4.3008	4.525091894	4.782709693	1.850591551	1.923700218
4.3776	4.445248796	4.51668347	1.671300341	1.675031319
4.4544	4.682951569	4.09398257	1.704498613	2.105537525
4.5312	4.583710725	4.464187606	1.880939038	1.975921431
4.608	4.733301863	4.272617659	1.875894889	1.95832937
4.6848	4.384778416	4.370094091	1.844365375	1.832303753
4.7616	4.422202941	4.246955174	2.278337698	1.898337249
4.8384	4.571724281	4.317585095	1.805789247	1.785163913
4.9152	3.804303741	4.348379218	2.169215388	1.914640009
4.992	3.841210584	4.295482811	2.737278127	1.483994
5.0688	3.853764402	4.311443342	2.055955677	1.828081822
5.1456	4.044193451	4.175392559	2.086395498	1.503084596
5.2224	4.013580747	4.381595199	2.058433451	1.695325529
5.2992	3.891052553	4.434981703	1.766409932	1.879139474
5.376	4.194364417	4.354494384	1.672709406	1.911820364
5.4528	3.826401519	4.129315405	1.853355766	1.599757066
5.5296	3.655326378	4.23918991	1.666459037	1.562874011
5.6064	3.595298818	4.278071074	1.591406473	2.096118197
5.6832	4.043138074	3.878923054	1.65584165	1.632771498
5.76	3.976340473	4.103907947	1.552686137	1.956008849
5.8368	3.71392698	4.319058969	1.631212562	1.823749518
5.9136	4.024135152	4.30944287	1.743710783	1.582369526
5.9904	4.395919256	4.398162158	1.553071945	2.238644253
6.0672	4.264039373	4.363249005	1.652087564	1.9963625
6.144	3.849206787	4.194955005	1.719477586	2.48783575
6.2208	4.145735695	4.047015692	1.735471367	2.375608313
6.2976	4.000794194	4.202122909	1.835219522	2.120159037
6.3744	3.719635599	4.255347978	1.784799062	2.195842748
6.4512	3.6440213	4.449905867	1.635694744	2.036601967
6.528	4.062415351	4.694213359	1.616350814	1.971449989

6.6048	4.351806434	4.553550666	1.837188953	2.025499548
6.6816	3.911661131	4.725671481	1.786716569	2.052445507
6.7584	3.843860039	4.718264855	2.157799117	1.987197042
6.8352	4.015353801	4.096175499	1.826338791	1.798376402
6.912	3.703913503	4.411081735	1.977599875	2.003307638
6.9888	3.997557471	4.148658314	1.783464556	1.984270552
7.0656	4.196455653	4.491435573	1.958984523	1.954180773
7.1424	4.055578866	4.748804557	1.72161524	2.024400307
7.2192	3.767933554	4.065482966	1.967337524	2.230929214
7.296	3.993803621	4.343425109	1.641950023	1.857892073
7.3728	4.280946819	4.200701332	1.793135529	2.157690772
7.4496	4.189462094	4.215346844	1.851435549	2.394781823
7.5264	3.971967492	4.134961904	1.829470999	2.172443389
7.6032	3.903662065	4.429401035	1.835774851	1.660732374
7.68	3.718323947	4.282539645	1.8018201	1.736096825
7.7568	3.536256356	4.264992976	1.732857654	1.835427964
7.8336	3.417930732	4.510961733	1.746910174	1.688925027
7.9104	3.597478526	4.606997972	1.681059759	2.131967365
7.9872	3.81220998	4.374443368	1.928709255	1.921247549
8.064	3.958548087	4.548755295	1.746900884	2.514710055
8.1408	4.016583179	4.516697098	2.316902573	2.462517672
8.2176	3.882718347	4.590177304	2.10920574	2.376363393
8.2944	3.894950156	4.704581083	2.134940905	2.423968497
8.3712	4.441809735	4.881558842	2.231087471	2.208809349
8.448	4.279030943	4.38886933	2.151454153	2.649925062
8.5248	4.634256647	4.83220073	2.138110602	2.424069526
8.6016	3.843320771	4.642116866	2.201981767	1.988119549
8.6784	3.85154183	4.574275162	2.042970774	2.047968329
8.7552	3.54358732	4.391849059	2.121493888	1.859137889
8.832	3.739798373	4.966398308	1.950152132	1.878839254
8.9088	3.770245418	4.852358891	2.245133292	2.19529012
8.9856	3.572029313	4.159081438	2.238952644	2.248110181
9.0624	3.391079731	4.380090685	2.150405506	2.369909547
9.1392	3.526683335	4.53072667	2.144372701	2.392528967
9.216	3.877334414	3.760255837	1.965839683	2.423488678
9.2928	4.061914111	4.049103377	2.091436352	2.760430027
9.3696	3.861427385	4.34323153	2.108640316	2.28682428
9.4464	3.638861817	3.933393934	2.176176439	2.256406599
9.5232	3.901129108	4.050937144	2.0732364	2.101408214
9.6	3.815632861	4.274310459	2.160093976	2.273750157
9.6768	4.593985059	4.186602462	2.043227603	2.241579743
9.7536	4.015669067	4.825439143	2.269464009	2.403104776
9.8304	4.122724975	4.787252177	2.126053773	2.093549205
9.9072	4.144863339	4.458960273	2.110593989	2.258758618
9.984	4.048622372	4.168871859	2.289612411	2.170040962

10.0608	3.661717927	3.837635993	2.367452283	2.023963895
10.1376	3.811642018	4.224062382	2.116638749	2.371292491
10.2144	3.925430037	4.151198217	2.330702732	2.286854102
10.2912	4.021819676	4.277064077	2.111082254	2.075109134
10.368	4.004826506	4.178624246	2.176744041	2.223916403
10.4448	4.534057568	4.07419186	2.318434994	2.646837674
10.5216	4.253131451	4.359333615	2.204159276	2.30647165
10.5984	4.236470629	4.283731741	2.380262317	2.33306286
10.6752	4.856568883	4.225827519	2.143841578	2.22215792
10.752	4.421124214	4.340282478	2.152182112	2.245425068
10.8288	4.245603149	4.097134442	2.185637142	2.289332491
10.9056	4.086066469	4.615186003	2.201155356	2.074411439
10.9824	4.261356581	4.936465642	2.197218241	2.278565085
11.0592	3.959621457	4.999462672	1.992924979	2.224644154
11.136	3.955928082	4.954946573	2.249732981	2.399484026
11.2128	4.302422655	4.3238447	2.176784427	2.696580109
11.2896	4.172620866	4.474705239	2.174796607	2.32048019
11.3664	4.266141882	4.366180089	2.225265361	2.377919766
11.4432	4.196187648	4.433829122	2.030483655	2.497563238
11.52	3.962596869	3.936589094	2.203010771	2.260892881
11.5968	4.093008825	4.37274163	1.935297793	2.156686596
11.6736	3.917380217	4.402596261	2.117925192	2.077182264
11.7504	4.073545445	4.316827076	2.178979932	2.150318018
11.8272	3.810241547	4.194342607	2.200938784	2.506206288
11.904	4.33084994	4.374974134	2.15585482	2.214368488
11.9808	3.781952796	4.66599821	2.295258345	2.387967993
12.0576	3.5542979	4.940206168	2.295534639	2.060387794
12.1344	4.375614599	4.619551496	2.195803746	2.156731915
12.2112	4.06356346	4.811343117	2.075156944	2.45791361
12.288	4.487901627	4.244851302	2.022584168	2.296069344
12.3648	4.131975806	4.616348125	2.17104017	2.278714076
12.4416	4.655610893	4.445048127	2.236285737	2.438718742
12.5184	4.746663718	4.273541762	1.905222505	2.303603686
12.5952	4.337953313	4.401421128	2.401599736	2.219556877
12.672	4.265916646	4.603687173	2.113634198	2.31242338
12.7488	4.612433032	4.3190261	2.286256279	2.526130967
12.8256	4.324146308	4.599133638	1.944803103	2.43071677
12.9024	4.480117506	4.685570049	2.034045519	2.336172938
12.9792	4.543615585	4.522448366	2.056713292	2.357274786
13.056	4.200391747	4.483781718	2.144046049	2.424003568
13.1328	4.194509445	4.194574367	1.912947236	2.338380077
13.2096	3.922151136	4.464815793	2.031201428	2.415453281
13.2864	4.090503377	4.727678072	1.921832665	2.220735919
13.3632	4.263817764	4.606687382	2.020812235	2.381364824
13.44	4.448475091	4.899574125	1.932702977	2.336524642

13.5168	4.209761104	4.482985148	1.961911583	2.326464062
13.5936	4.222207639	4.197240105	2.226560733	2.504451936
13.6704	4.355353346	4.723906683	1.963476109	2.687295292
13.7472	4.195284204	4.670726777	1.924515667	2.610526169
13.824	4.508291968	4.918823065	1.864152351	2.434693904
13.9008	4.836563586	5.019448155	2.050093994	2.293808347
13.9776	4.643472025	4.713842184	2.155671712	2.245762684
14.0544	4.177351103	4.379810298	2.005572558	2.655225466
14.1312	4.738881332	4.330100143	1.896522218	2.577203202
14.208	4.150786292	4.268242418	2.080822286	2.177364269
14.2848	4.405875544	4.369150411	2.055158179	2.299147473
14.3616	3.970491533	4.503363766	1.88385894	2.469662457
14.4384	4.363095885	5.023583015	1.861316831	2.545006283
14.5152	4.628290964	4.627460259	1.668816794	2.373325984
14.592	4.63679081	4.656821157	2.22730384	2.372883037
14.6688	4.481995046	4.54313292	1.888131992	2.253764265
14.7456	4.639263544	4.379684304	2.204880935	2.633491457
14.8224	4.578881809	4.663874518	2.125499779	2.476907076
14.8992	4.187751784	4.456341221	1.927733485	2.70165981
14.976	3.950814898	4.571242844	2.139300193	2.243050757
15.0528	4.662960923	4.554054556	2.185555286	2.357113285
15.1296	4.754921612	4.36375095	2.060228187	2.424687532
15.2064	4.565816836	4.706110414	2.133572798	2.346490001
15.2832	4.325502809	4.636303177	2.168234771	2.340025744
15.36	4.005012915	4.557106907	2.145090523	2.386946486
15.4368	4.686511477	4.466748703	2.155177375	2.488661991
15.5136	4.427530865	4.046932189	2.024059391	2.307132379
15.5904	4.243189374	4.046277259	2.085855232	2.135555286
15.6672	4.406365618	4.147144414	2.163200123	2.310228187
15.744	4.588612962	4.645250105	2.126409974	2.383572798
15.8208	4.480496753	4.439322878	2.11695301	2.418234771
15.8976	4.375211763	4.658296332	2.162349656	2.162020559
15.9744	4.645249908	4.410864981	2.274179843	2.301203336